Forest Ecology and Management 580 (2025) 122542

Contents lists available at ScienceDirect

Forest Ecology and Management

journal homepage: www.elsevier.com/locate/foreco

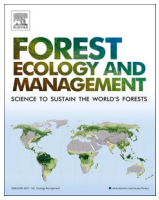

Changes in wood density, growth, and carbon storage of the main stem of planted white spruce (*Picea glauca*) after commercial thinning

Dipak Mahatara [a,*], Julie Barrette [b], Boris Dufour [a,c], Luc Sirois [a], Alexis Achim [d], Robert Schneider [a]

[a] *Département de biologie, Chimie et Géographie, Université du Québec à Rimouski, 300 allée des Ursulines, Rimouski, QC G5N 1E8, Canada*
[b] *Direction de la recherche forestière, Ministère des Ressources naturelles et des Forêts du Québec, 2700 rue Einstein, Québec, QC G1P 3W8, Canada*
[c] *Centre d'expérimentation et de développement en forêt boréale, 537 boulevard Blanche, Baie-Comeau, Québec, QC G5C 2B2, Canada*
[d] *Centre de recherche sur les matériaux renouvelables, Département des sciences du bois et de la forêt, Pavillon Abitibi-Price, 2405 rue de la Terrasse, Université Laval, Québec, QC G1V 0A6, Canada*

ARTICLE INFO

Keywords:
Thinning
CO_2 sequestration
Ring-density modeling
Crop tree release
Within-tree density variation
White spruce

ABSTRACT

Commercial thinning, often included in silvicultural scenarios applied to plantations, influences tree growth and wood properties and, consequently, can modify the carbon sequestration rate of tree stems. The present study considered the wood density variations within and between tree stems to estimate carbon dioxide (CO_2) sequestration in the stem under four treatments—control, thinning from below, early release of 50 crop trees per hectare, and 100 crop trees per hectare—conducted in white spruce (*Picea glauca*) plantations in eastern Quebec. The plantations dating from 1990 were thinned in 2008. First, disk samples collected in 2021 from 140 trees across the four thinning intensities were used to construct a ring-density model following thinning. The plot inventory data from 2008, 2014, and 2021, combined with the ring-density model, were then used to estimate individual tree carbon sequestration, which was summed at the plot level. We found that (1) ring density displayed higher values near the pith, followed by a rapid decline, after which ring density slightly increased toward the bark; (2) thinned and control treatments showed similar average ring-density chronologies throughout the study period, constraining the generalization of post-thinning ring-density trends; and (3) thinned plots exhibited lower tree CO_2 sequestration rates than control plots, with estimates of 5.17, 5.35, 4.75, and 5.84 $t \cdot ha^{-1} \cdot year^{-1}$ for 100 crop trees per hectare, 50 crop trees per hectare, thinning from below, and the control respectively. This study provides insights into how thinning impacts carbon dynamics in the tree stems of young stands, which can be used to weigh the trade-offs between active management and carbon storage.

1. Introduction

Forests store 40–60 % of global terrestrial carbon and play a crucial role in the global carbon cycle (Nabuurs et al., 2007; Pan et al., 2011). Intensive forest management is considered the third-largest natural pathway to mitigate climate change (IPCC, 2023), although it has yet to be fully quantified. A better understanding of forest carbon dynamics in diverse management scenarios is crucial for advancing sustainable practices and improving projections of future atmospheric CO_2 concentrations.

Under certain circumstances, well-managed forest ecosystems can serve as carbon sinks (Jandl et al., 2007; Noormets et al., 2015; Ontl et al., 2020; Moreau et al., 2022). Among different forest management practices, thinning is the most important and widely used silvicultural tool that directly influences stand structure and, in turn, tree growth, wood quality, and carbon content (Ruiz-Peinado et al., 2013; Russo et al., 2019). In general, the radial growth and earlywood percentage of conifer species are expected to increase after thinning (Zhang, 1995; Tasissa and Burkhart, 1997; Mäkinen et al., 2002). Thinning reduces competition among the remaining trees and promotes an increased availability of water, nutrients, and solar radiation, thereby enhancing the growth and vigor of residual trees (Eriksson, 2006; Geng et al., 2021). Several studies suggest that thinning may contribute to higher carbon sequestration rates within the thinned stand by favoring the increased growth of residual trees and enhancing undergrowth vegetation and regeneration (Briceño-Elizondo et al., 2006; Garcia-Gonzalo

* Corresponding author.
E-mail address: dipak.mahatara@uqar.ca (D. Mahatara).

https://doi.org/10.1016/j.foreco.2025.122542
Received 26 September 2024; Received in revised form 26 January 2025; Accepted 27 January 2025
Available online 4 February 2025

et al., 2007; Zhang et al., 2019). In contrast, some studies have shown that thinning significantly alters stand density, stimulates microbial activity and litter decomposition, and consequently decreases carbon storage (Kariuki, 2008; Ruiz-Peinado et al., 2016; Lin et al., 2018; Gong et al., 2021). Moreover, some studies on thinning from below, when the treatment is implemented early in the stand's development, have observed that trees grown at lower densities exhibit increased growth rates, which can sustain or even enhance carbon storage (Hoover and Stout, 2007; Dwyer et al., 2010). These findings suggest that thinning indeed increases the growth and quality of individual trees, but it does not always lead to an increase in the total carbon storage of a stand. Moreover, the extent of post-thinning carbon storage is intricately influenced by factors such as the intensity of thinning and its type (Hoover and Stout, 2007), tree species and their status in the stand (Peltola et al., 2002; Zhang et al., 2018), age during thinning (Schroeder, 1991) and environmental conditions (Downes and Drew, 2008; Gonzalez-Benecke et al., 2010). These multiple influences make it challenging to generalize the consequences of thinning on carbon dynamics.

Forest carbon stocks can be divided into three main pools: (i) biomass (above- and belowground); (ii) deadwood and litter, which includes both woody detritus and forest floor components; and (iii) soil organic matter (IPCC, 2003). As noted by Bolstad and Vose (2005) and Kurz et al. (2013), most ecosystem carbon is stored in the biomass pool (30 %) and mineral soil (40 %). Among all carbon pools, the aboveground carbon pool, in particular the tree stem, varies significantly with silvicultural treatments, making it a key indicator for studying carbon dynamics following forest management (Jenkins et al., 2003; Schaedel et al., 2017). Despite the destabilizing effects of thinning on soil structure and function—such as water movement and retention (Bronick and Lal, 2005)—evidence suggests that soil carbon pools typically remain stable and show little variation relative to aboveground carbon pools (Jurgensen et al., 1997; Johnson and Curtis, 2001; Nave et al., 2010; D. Zhou et al., 2013). Moreover, the deadwood carbon pool is altered by thinning, especially in temperate forests, where decomposition occurs at a slower rate (Harmon and Hua, 1991). In old-growth forests, woody debris and forest floor carbon pools are substantial and remain largely unaffected by stand density management (Franklin et al., 2002).

Generally, the carbon content of the aboveground woody biomass is determined by multiplying dry biomass by a carbon conversion factor (IPCC, 1990; Pan et al., 2011; Nizami, 2012). A value of 0.5 has widely been used (Hollinger et al., 1993; Matthews, 1993; Brown, 2002; Chave et al., 2005; Zhang et al., 2015; Fahey et al., 2010). Dry biomass can be estimated either using biomass equations or by multiplying the cubic volume by wood density for a given species (Handbook, 1999; Jenkins, 2004). However, these biomass equations assume the same dry weights for trees of the same size, ignoring the effects of wood density variations associated with age, treatment, and the growing environment.

Basic wood density refers to the ratio of oven-dried weight to green volume and is recognized as a primary indicator of wood quality (Ortega Rodriguez and Tomazello-Filho, 2019). Distinct wood density patterns exist within the stem radially and along the bole, both among individuals and species (Wiemann and Williamson, 1989; Muller-Landau, 2004). Ignoring this variability can lead to substantial inaccuracies in estimates of carbon (Laurance et al., 2007). Variation in the radial and vertical dimensions within the stem can become more evident with changes in forest management practices (Zubizarreta Gerendiain et al., 2007; Downes and Drew, 2008; D'Amato et al., 2011). In pioneer and early successional species, wood density typically increases from pith to bark. Conversely, in late-successional species, wood density tends to decrease from pith to bark, reflecting an adaptive strategy to manage complex loading patterns (Van Gelder et al., 2006). Vertical variations in wood density are explored less than radial patterns because of the challenges of acquiring samples. Generally, wood density decreases from the tree's base to its top, attributed to the changing proportion of juvenile wood (Zobel and Van Buijtenen, 2012). Wood density values reported in the literature are often obtained from a single defect-free core sample at breast height (BH; Williamson and Wiemann, 2010). Thus, the use of generic wood density values of tree species can produce misleading carbon estimates, as the average might not capture the full complexity of the wood density variability within a tree (Muller-Landau, 2004; Repola, 2006; Wiemann and Williamson, 2014; Bastin et al., 2015).

There has long been an interest in the development of models to predict annual ring density (RD) as a means of enhancing our understanding of the consequences of silvicultural interventions on wood quality. These models can be used to convert volume to dry biomass and subsequently to carbon and energy content of a stem through the use of volume equations, yield tables, and growth models. Most previous studies have applied cambial age as a key variable to characterize RD (Ikonen et al., 2008; Schneider et al., 2008; Ivković et al., 2013; Auty et al., 2014; Kimura and Fujimoto, 2014; Xiang et al., 2014), as it captures the complexity of tree growth patterns and physiological changes. Nevertheless, applying models reliant on cambial age can be challenging when cambial age is not available (e.g., inventory data without increment cores).

Various thinning strategies are used to achieve diverse forest management objectives (Ashton and Kelty, 2018). Since 2014, forest management plans in Quebec, Canada, must reduce the differences between managed and unmanaged forests to maintain natural ecosystem properties—composition, structure, and function (Gagné et al., 2016). Commercial thinning by early crop tree release (CTR) has been recommended as a way to initiate structural conversion and accelerate the development of uneven-aged forest stands over the long term (Singer and Lorimer, 1997; Gagné et al., 2016, 2019). CTR provides density control at the individual level to release certain dominant trees from competition (commonly between 50 and 200 trees·ha^{-1}). Either fixed radius (e.g., 3 m) or free on two or four sides is used in the province of Quebec (Grenon et al., 2007; Miller et al., 2010). Although a growing concern exists in regard to growth and stand structure following CTR (Trimble, 1971; Ward, 2002, 2013; Laflèche et al., 2013; Dupont-Leduc et al., 2020), the short- and long-term effects of CTR on forest productivity, wood quality, and annual carbon uptake potentiality remain poorly understood.

In this regard, the general objective of this study is to investigate the effect of CTR on the wood density of white spruce (*Picea glauca* (Moench) Voss), the annual aboveground stem volume increment, and the associated carbon uptake as part of a thinning trial in plantations that follows a randomized block design having four intensities (Gagné et al., 2016; Dupont-Leduc et al., 2020): 1) control, only the skid trails were harvested; 2) thinning from below, uniform removal of small, diseased, or deformed stems, with a targeted removal of 30 % basal area; 3) 50 CTR: early release of 50 crop trees per hectare from competition on all sides within a 3 m radius from the bole; and 4) 100 CTR, early release of 100 crop trees per hectare from competition on all sides within a 3 m radius from the bole. Our study addressed these specific questions: (1) Does thinning lower the wood density along the stem of white spruce? (2) Does the intensity of thinning affect the CO_2 sequestration capacity of individual trees and stands in their stems? (3) Is it important to take wood density variations into account when calculating the amount of carbon sequestered in the stem of trees following thinning? To answer these questions, we first developed a mixed-effects model for predicting RD following thinning, applied the established model to estimate the RD of trees in the permanent sample plots, and subsequently calculated CO_2 sequestration in the stem on the basis of volume and the predicted density. The concept of CTR has been recently applied to softwood stands in eastern Canada, and determining the effects of this innovative approach on carbon density can assist in evaluating the applicability of CTR for global carbon mitigation. Additionally, this integrative methodological approach helps to reduce the uncertainties in estimating the carbon content of tree stems.

2. Materials and methods

2.1. Sampling design

The study used a thinning trial located in the Lower St. Lawrence region of Quebec, Canada (47.0°–48.5°N, 68.0°–69.0°W). The climate is characterized by a mean annual temperature of 2.0 °C, an average annual precipitation of 1032 mm, and a growing season length that ranges between 130 and 140 days with about 92 frost-free days (Environnement Canada, 2015).

The trial, established in 2008, consists of two white spruce plantation stands (Lechasseur and Humqui), planted in 1982 and 1984, respectively. Before planting, the sites were prepared by raking, and herbicides were applied three years after planting. The trial follows a randomized block design with plantation sites as blocks (Dupont-Leduc et al., 2020) and includes four thinning treatments within each block: 1) control, 2) thinning from below, 3) thinning with 50 CTR per hectare, and 4) thinning with 100 CTR per hectare. All four thinning intensities have five replicates for a total of 20 experimental units (EU; 99 × 76 m, 7 500 m^2) per block. Furthermore, each EU was subdivided into three experimental subunits of around 2500 m^2. In one of these subunits, a permanent sample plot with an approximate dimension of 33 x 15 m (area 379 −633 m^2) was established six years after thinning (i.e., in 2014).

The trees removed during thinning from below had a diameter at breast height (DBH; in cm, at 1.3 m above the ground) less than 12 cm and at least one 2.44 m log with a top-end outside bark diameter of at least 9.1 cm (Gagné et al., 2016). In the CTR, the crop tree was freed from all the competitors. A tree was considered a competitor when its branches touched the crop tree and were at least half the height of the crop tree. A tree was considered a crop tree when it 1) was dominant or codominant; 2) was vigorous with no signs of defoliation; 3) had a branch of maximum diameter < 2 cm on the first 2 m of the bottom log; 4) had a crown with a regular form and no defects; and 5) maintained a live crown ratio of 40 %–60 % (Gagné et al., 2016).

2.2. Data collection

From all 40 permanent sample plots, the DBH of all trees (≥5 cm) and the total tree height (m) of every 15th tree were measured in 2014 and 2021. As the permanent sample plots were established in 2014, tree-level information before the thinning year was not available. Increment cores collected at BH in 2014 from all the trees in the permanent sample plots were used to interpolate the DBH at the time of thinning (Dupont-Leduc et al., 2020).

Three to four white spruce trees were selected for destructive sampling from each EU. For this, three points were randomly positioned in one of the two subunits that did not contain the permanent sample plot. In the field, the closest crop tree and codominant competitor to point 1 were selected. Likewise, a codominant tree closest to point 2 and an intermediate tree with a DBH ≥ 9.1 cm closest to point 3 were chosen. In this way, 40 codominant trees and 40 intermediate trees from all 40 EUs were sampled. We only sampled 30 crop trees and 30 codominant competitors from the 40 EUs (10 crop trees and 10 codominant competitors from the EUs of 50 CTR·ha^{-1} and 100 CTR·ha^{-1}, and 10 crop trees and 10 codominant competitors from both the control and thinning from below EUs). This was done to maintain the same proportion of crop trees per treatment, as the individual-level release was identical in the 50 and 100 CTR·ha^{-1} treatments, differing only in the number of crop trees treated (e.g., crop trees released in the 50 and 100 CTR treatments were freed from competition in the same way). One hundred and forty trees were thus destructively felled in the summer of 2021. The DBH of the sample trees was measured, and after felling, total tree height and trunk diameter at an interval of 1 m from base to top of the tree were measured. Also, the DBH, azimuth, and distance of all trees in a 5 m radius around the sample trees were recorded. Disks (2 cm thick) were cut from five positions along the stem at 0 % tree height, BH (1.3 m), 25 % tree height, 50 % tree height, and 75 % tree height. On each disk, north was indicated.

2.3. Wood density measurements

The collected disks were stored in a conditioning room at 22–23 °C and 58 % relative humidity until a constant weight was reached, implying an approximate moisture content of 12 % (ISO 554, 2002). Following this step, the cross-sectional disks were passed through a medical CT scanner (Somatom Definition AS+128; Siemens Healthcare GmbH, Erlangen, Germany) located at the Institut national de la recherche scientifique, Centre Eau Terre Environnement, Quebec City, Canada. The x-ray tube of the CT scanner was set to operate within an energy range of 70–140 kV and a current ranging from 300 to 700 mA.

We applied the R CTRing package (Mahatara et al., 2024) to extract the ring-level information from the CT images. In summary, the package adapts the Hough Transform method to locate the pith position and modified version of the *getBorders* function from the R xRing package (Campelo et al., 2019) for ring segmentation of the selected path. Two pith-to-bark density profiles were obtained from two radial directions (north and east) for each disk. The profile paths were adjusted, if necessary, to avoid knots, cracks, or unclear ring boundaries. We manually counted the number of rings on each disk, and rings were added or removed accordingly, using the graphical user interface (GUI) of the CTRing package. We did not include the outermost ring (ring formed in the year 2021) in the density profile, given its incomplete formation. The yearly RW and RD were averaged over each profile to obtain one series of RW and RD for each disk. The acquired series of RW were then cross-dated within individual trees and across the entire experimental unit using the *corr.rwl.seg* and *ccf.series.rwl* functions available in the dplR package (Bunn, 2010). We excluded damaged and broken disks from scanning; therefore, our data set consisted of density profiles from 678 disks containing 13,254 annual rings. The obtained density values were relative density or specific gravity, defined as the ratio of a substance's density to that of pure water at 4 °C, which were then expressed as mass at 12 % divided by volume at 12 %. A summary of tree- and ring-level characteristics before and after thinning is given in Table 1.

2.4. Predicting post-thinning ring-density profiles

Unlike many similar studies (Ivković et al., 2013; Auty et al., 2014; Filipescu et al., 2014; Xiang et al., 2014; Franceschini et al., 2018), we chose years after thinning as the primary predictor variable rather than cambial age to model mean RD. This choice was made because the RD model was to be applied to data from the permanent sample plots to assess CO_2 sequestration following thinning, and the age of the individual trees is unknown. We thus considered 2009 as the first year after thinning, and this progression culminated with 2020 as the twelfth year. Rings formed in the year of thinning and before the thinning were omitted from the final modeling data set. The model was thus established by running RD data derived from a total of 7804 annual rings of 678 disks from 140 trees.

We applied mixed-effects models to align with the nested structure of the data: disks nested within trees, trees nested within plots, and plots within sites. We used the *lmer* function from the lme4 package (Pinheiro, 2009) in R, using the maximum likelihood method to fit the models. At first, we examined various variance–covariance structures of random effects with all possible combinations of hierarchical levels and found disks nested within trees as the best structure. Second, for model specification, we used a two-stage modeling approach to account for the distinctive trends in the RD of individual disks. In the first stage, we developed a disk-level model (Eq. 1) with year after thinning as a predictor variable, and in the second stage, we regressed the parameters of the disk-level model with all possible tree- and ring-level covariates

Table 1
Tree- and ring-level characteristics of sampled trees before and after thinning treatment.

Block	Treatment	Relative ring density		Ring width (mm)		DBH in 2021 (cm)	Height in 2021 (m)	Competition index
		Before thinning	After thinning	Before thinning	After thinning			
HU	100 CTR	0.395 (0.089)	0.360 (0.044)	3.58 (1.17)	2.81 (1.12)	18.50 (4.38)	13.09 (2.09)	1.20 (0.26)
	50 CTR	0.387 (0.078)	0.343 (0.043)	3.56 (1.11)	2.79 (1.14)	16.76 (4.16)	12.89 (2.12)	1.11 (0.27)
	Below	0.383 (0.089)	0.346 (0.053)	3.60 (1.27)	2.94 (1.15)	18.37 (4.55)	13.11 (2.66)	1.10 (0.35)
	Control	0.397 (0.096)	0.356 (0.053)	3.75 (1.22)	2.86 (1.15)	17.50 (4.35)	13.26 (2.53)	1.02 (0.26)
LE	100 CTR	0.378 (0.080)	0.357 (0.054)	3.85 (1.41)	2.69 (1.18)	19.28 (4.89)	13.70 (2.38)	0.94 (0.44)
	50 CTR	0.377 (0.081)	0.353 (0.052)	3.64 (1.32)	2.48 (1.01)	16.65 (4.84)	12.84 (1.71)	0.93 (0.31)
	Below	0.379 (0.071)	0.356 (0.044)	3.88 (1.18)	2.59 (1.02)	20.35 (4.61)	13.94 (2.21)	0.99 (0.25)
	Control	0.378 (0.080)	0.354 (0.056)	3.89 (1.26)	2.61 (1.05)	18.90 (4.54)	13.75 (1.83)	1.03 (0.27)

Values shown are the mean and standard deviation in parentheses. HU and LE denote the sites Humqui and Lechassseur, respectively.

(Table 3). Subsequently, the variance–covariance structure was added to Eq. 1, and the parameters α_0, α_1, and α_2 of Eq. 1 were substituted by their respective linear model developed in stage 2, resulting in the formulation of the final model (Eq. 2). The summary of the parameter values obtained from the disk-level model can be found in Table 2, and the definitions and abbreviations used for the candidate tree- and ring-level covariates can be found in Table 3. Detailed information for each step of model development is available in the supplementary information (Appendix A).

$$RD_{ijk} = \alpha_0 + \alpha_1 \bullet \ln(TY_{ijk}) + \alpha_2 \bullet TY_{ijk}^2 + \varepsilon_{ijk}, \quad (1)$$

where TY_{ijk} denotes the year after thinning for the k^{th} annual ring of the j^{th} disk from the i^{th} tree, and α_0, α_1, and α_2 are the parameters to be estimated.

$$RD_{ijk} = \left(\beta_0 + \beta_1 \bullet DBH_i^2 + \beta_2 \bullet \sqrt{RW_i} + \beta_3 \bullet h_{disk_{ij}}\right) + \left\{\left(\beta_4 + \frac{\beta_5}{DBH_i^2} + \beta_6 \bullet h_{disk_{ij}}\right) * \ln(TY_{ijk})\right\} + \{(\beta_7 + \beta_8 \bullet CI_i + \beta_9 \bullet h_{disk_{ij}}) * TY_{ijk}^2\} + \mu_i + \mu_{ij} + \varepsilon_{ijk}, \quad (2)$$

where β_0, β_1, β_2, β_3, β_4, β_5, β_6, β_7, β_8, and β_9 are the parameters to be estimated, μ_i represents the tree random effect, μ_{ij} is the disk nested in tree random effect, and ε_{ijk} is the error term.

2.5. Assessing post-thinning CO_2 sequestration

2.5.1. Mean post-thinning wood density

The RD model uses year after thinning, RW, h_{disk}, DBH, and CI after 12 years of thinning as input variables (Eq. 2). The individual RW was obtained from the PSP data by dividing the observed growth by the number of years in the interval for each period (period 1: RW = ($DBH_{2014} - DBH_{2008}$)/ (2 × 6), period 2: RW = ($DBH_{2021} - DBH_{2014}$)/ (2×7)). CI was calculated as presented in Table 3, i.e., the ratio between DBH_{2021} and the mean quadratic DBH in 2021. Finally, the RD for each ring was calculated for five-disk heights (0 %, 1.3 m, 25 %, 50 %, and 75 % total height of the tree in 2021).

Furthermore, the average wood density per growth period (2008–2014, 2014–2021) was calculated as follows.

Table 2
Descriptive statistics for the parameters α_0, α_1, and α_2 obtained by fitting Eq. 1 to 678 individual disks.

Parameters	Mean (Range)
α_0	0.325 (0.179–0.467)
α_1	2.227 (−0.28 to 123.37)
α_2	0.00043 (−0.00075 to 0.00175)

Table 3
Definitions of the abbreviations of the candidate variables used to develop the final ring-density model.

Abbreviations	Description
DBH	Tree diameter at breast height (in cm)
Ht	Total height of the tree (in m)
RW	Average ring width of the tree at breast height (in mm)
h_{disk}	Disk position along the stem from stem base as a factor
CI	Quadratic diameter competition index, $\frac{DBH_i}{\sqrt{\frac{1}{N}\sum_{j=1}^{N}\left(DBH_j^2\right)}}$, where DBH_i is the diameter at breast height (DBH) of the subject tree (in cm), DBH_j is the DBH of *j*th neighboring tree (in cm), and *N* is the total number of neighboring trees in a 5 m radius around the subject tree.
D_{class}	Dominance or social class of the tree as a factor

1. Between the rings of one disk for each period
   The outermost ring contributes more to the volume than the innermost ring, rendering a simple averaging of densities between the rings imprecise. To address this, we quantified the ring area at each disk height for each year after thinning and used these areas (or increments) as weights to compute the average density between the rings. For the disk at BH (BH, 1.3 m), we calculated the area increment for each year by using the DBH measured in years 2008, 2014, and 2021. This calculation enabled us to compute the area-weighted density of each ring at BH for each growth period. For the disks other than at BH, the stem increment data were unavailable, so we used the ring area per year for all disks from the sample trees (140 trees). We determined the area weight for each year by averaging all the disks at each height and subsequently calculated the weighted mean wood density per growth period and height.
2. Between the disks of one tree for each period

Given that different disk heights represent varying proportions of the tree volume, we assigned weights to each disk on the basis of their respective heights. To obtain the weight, we used the taper measurement of our samples. For this, we first defined the proportions of tree height represented by each disk: disk from 0 % height (0–0.65 m), disk from BH (0.65–1.95 m), disk from 25 % height (1.95 m to 37.5 % of total height), disk from 50 % height (37.5–62.5 % of total height), and disk from 75 % height (62.5 % of total height to the top of the tree). The volume percentage of each section was then obtained and averaged over all the sample trees. Finally, we used the average volume percentages as a weight for the respective disks and obtained the average wood density for the two growth periods of each tree.

2.5.2. Volume increment and CO_2 sequestration of the main stem

As not all tree heights were measured, a height − DBH equation (Eq. 3) based on Fortin et al. (2009) was calibrated for each block, treatment, and year (Appendix B). As no height measurements were available for 2008, we applied the height – DBH equation calibrated for 2014 to the

2008 data.

$$Ht_i = a + b \bullet \ln(DBH_i + 1) + c \bullet \ln(DBH_i + 1)^2 + \varepsilon_i \quad , \tag{3}$$

where a, b, and c are the model parameters.

Tree volume for each inventory year was calculated from the measured DBH in 2008, 2014, and 2021, and we estimated height from Eq. 3 in combination with the volume equation (Eq. 4) developed by Prégent et al. (2010). The summary statistics of the DBH and height for all three inventoried years are presented in Table 6.

$$V_i = 0.0344 \bullet DBH_i^{1.8329} \bullet Ht_i^{1.1793} \quad , \tag{4}$$

where V_i is the total tree volume without bark (dm^3).

Finally, the tree-volume increment was obtained by subtracting the volume at time $t+1$ from that at t. Stem C-sequestration was then estimated for each tree as (Eq. 5):

$$C_{seq_{ip}} = 3.67 \bullet (V_{ip} \bullet \rho_{ip} \bullet E \bullet C_0) \quad , \tag{5}$$

where $C_{seq_{ip}}$ is the amount of CO_2 sequestered in the stem (kg), V_{ip} is the volume increment of the stem (m^3), and ρ_{ip} is the mean wood density ($kg \cdot m^{-3}$) of tree i for the growth period p. The term E denotes the density conversion factor—to convert wood density at 12 % moisture content to a basic wood density, we applied a constant value of 0.828 (Vieilledent et al., 2018)—and the term C_0 denotes the coefficient of carbon content; to convert dry biomass to carbon, we applied a constant value of 0.5. Finally, to determine the equivalent amount of CO_2, we multiplied the carbon content by a stoichiometric conversion factor of 3.67 (44/12).

The effects of the stand density index (SDI), thinning type (stand structure), and growth period on stand-level variables (volume increment and CO_2 sequestration) were analyzed using analysis of variance (ANOVA). SDI (Eq. 6) characterizes the density of stands on the basis of a quadratic mean diameter (d, in cm) and the number of trees per hectare (N) by calculating the number of stems per hectare with a mean diameter of 25 cm (Pretzsch and Biber, 2005). There was a high degree of correlation between SDI and thinning types; thus, we did separate analyses: one for stand-level variables vs. SDI and another for stand-level variables vs. thinning type. The site effect was also considered as blocks and thus added as a fixed term.

$$\mathrm{SDI} = N. \left(\frac{25}{d}\right)^{-1.605} \quad . \tag{6}$$

To assess the robustness of the average wood density at BH, we calculated total CO_2 sequestration per hectare over the 13 years studied by using within-tree density variations (actual CO_2 sequestration) and compared this value with that obtained using the average wood density at BH of this study. To provide evidence for the necessity of accounting for the effects of treatments and growing conditions in carbon estimation, we compared the actual CO_2 sequestration with values obtained using the published wood density of white spruce ($412\ kg \cdot m^{-3}$; De Araujo et al., 2015).

3. Results

For the 13,254 annual rings assessed, the relative RD ranged from 0.198 to 0.724, with a mean value of 0.366. There was a negative correlation between relative RD and annual RW, and this correlation was more pronounced before thinning (−0.50 and −0.39 before and after thinning, respectively). When averaging the pith-to-bark density profiles for the five different disk heights, we observed higher mean relative RD near the pith with a rapid decrease followed by a gradual increase toward the bark (Fig. 1A). This observed trend was consistent across all social classes (Fig. 1C) and thinning types (Fig. 1E). In the vertical direction, the mean relative density remained almost constant up to 50 %-disk height (0.364, 0.362, 0.359, and 0.361 for disk heights 0 %, BH, 25 %, and 50 %, respectively), with a slight increase observed at the topmost disk (0.373) (Fig. 1G). For a given growth year, intermediate trees exhibited higher mean relative RD (0.390), whereas the other three dominance classes had a nearly identical average relative RD (0.362, 0.357, and 0.358 for codominant, competitor, and crop trees, respectively) (Fig. 1C). The tree growth rate and average relative RD in both study blocks remained consistent between the control and thinned stands, showing a slow rise after thinning. The average relative RD chronologies within the thinned and control stands displayed increased variability near the pith, which gradually followed an identical trend after a few years. Eventually, four to five years after thinning, control stands showed a slightly higher relative RD value than in the thinned plots (Fig. 1E).

3.1. Model fitting

Approximately 5 % of RD profiles showed a consistent increasing trend, whereas the remaining 95 % showed no discernible systematic trend in density within their respective RD profiles. The accuracy of the disk-level models (stage 1) was evaluated by comparing predicted and observed values and by fitting model curves to their respective observed density profiles. The curves for the density profiles of individual disks were unbiased, indicating the effective representation of data patterns by Eq. 1 (not shown). The precision of the disk-level model is highlighted by root mean square error (RMSE) of 0.015, mean absolute error (|ME|) of 0.012, and absolute percentage mean error (|ME| %) of 3.57 %, all of which were calculated as averages of the 678 disks (Table 4).

The final model (stage 2, Eq. 2) showed that RD can be best described by adding ring width (RW at BH), disk-level (disk height) and tree-level covariates (DBH and competition index (CI)) as fixed terms and disk nested within the tree as a random term. The fixed effects parameter estimates and standard deviation of the random effects for the final model are presented in Table 5. The prediction of RD using the final model initially resulted in a 38 % explained variability, which significantly increased to 76 % with the inclusion of random effects. Error statistics obtained for the final model were 0.025, 0.018, and 5.23 % for RMSE, |ME| , and |ME| %, respectively (Table 4). The plot of the standardized residuals indicated no obvious residual trend in predicted RD (Fig. 2). The variance components of the random effects in the final model accounted for approximately 39 % and 24 % of the total variance at the tree and disk levels, respectively, leaving the remaining 37 % attributed to residuals (Table 5). Additionally, the final model's predicted average RD (0.354) closely approximated the observed post-thinning average RD (0.353), aligning well with the observed RD trends (Fig. 1). The trends showed a slight increase in RD with years after thinning for disks at 0 % and 25 % tree height and those at BH. Conversely, disks at 50 % and 75 % total height showed a decreasing trend followed by an increase (Fig. 1B). The average values predicted for RD on the basis of the final model were also higher for intermediate trees than for the other three dominance classes (Fig. 1D). Interestingly, the trees in the intermediate class required an additional few years following thinning to reach the lowest mean RD, whereas the other three dominance classes displayed a gradual post-thinning increase (Fig. 1D) from the first year. Finally, thinning intensity did not significantly improve the model's fit statistics (not shown). The average RD chronologies following thinning showed initial stability for the first few years, followed by a gradual increase for all the thinned and control stands (Fig. 1F). Moreover, a consistent increase in RD was observed after thinning for a given RW (Fig. 1H).

3.2. Tree volume and CO_2 sequestration

Before thinning, the average basal area in the plots ranged from 26.72 to 29.22 $m^2 \cdot ha^{-1}$ (Dupont-Leduc et al., 2020). Following thinning, basal area varied from 21.52 to 29.22 $m^2 \cdot ha^{-1}$, and the total standing volume ranged from 91.58 $m^2 \cdot ha^{-1}$ in the thinning from below

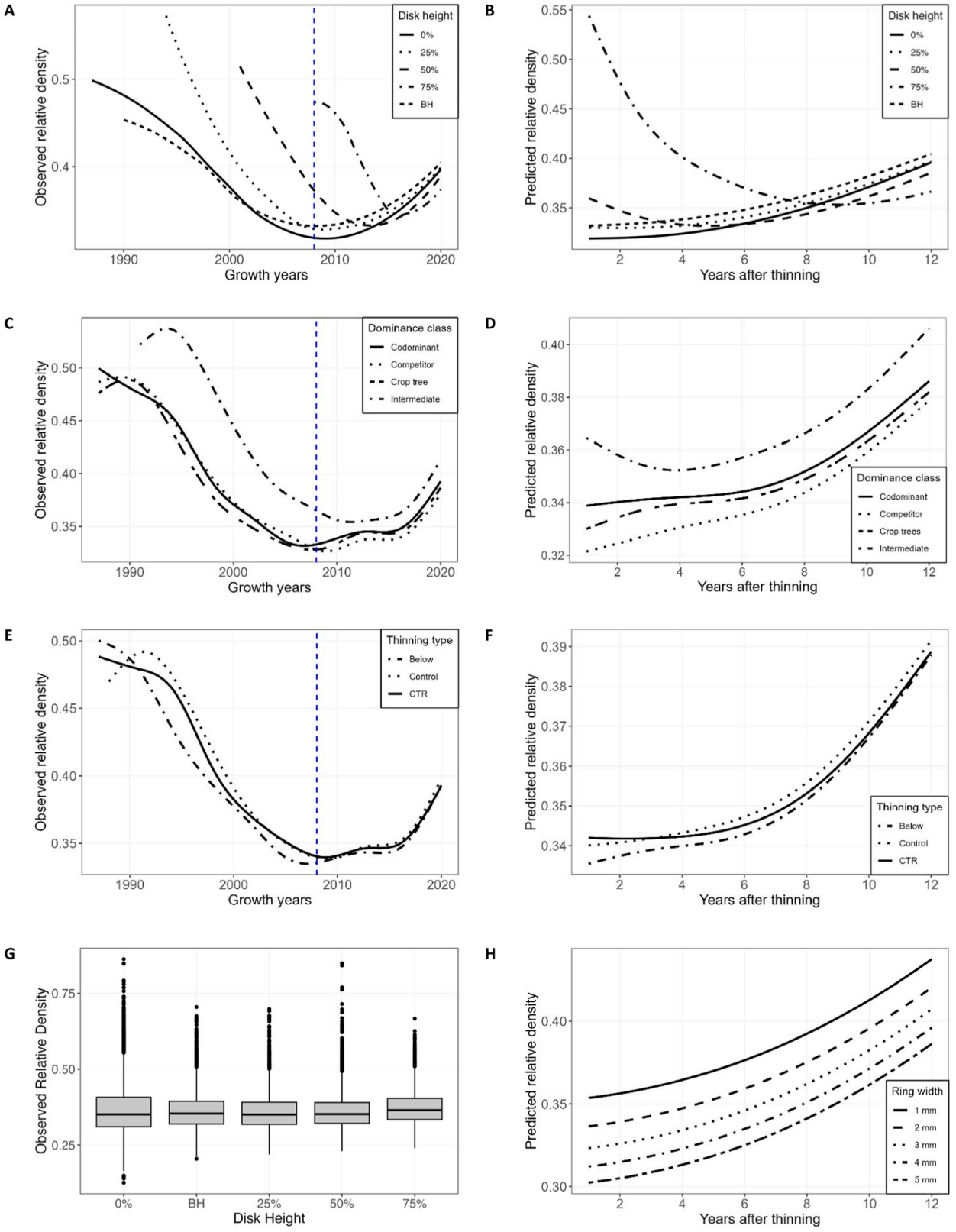

Fig. 1. Model predictions for the relative density of different disk heights, social or dominance classes, thinning types, and ring widths. Plots A, C, and E denote the observed spline-smoothed relative density of the annual rings plotted against disk height, social/dominance class, and thinning type, respectively; plot G denotes the axial pattern of observed relative density; plots B, D, F, and H denote the predicted relative density with years after thinning from final model (Eq. 2) for different disk heights, social/dominance classes, thinning types, and ring widths, respectively. To plot the predicted curves, we set all remaining tree-level and disk-level variables to their respective mean values. The blue vertical dotted line in the plots of the left panel represents the year of thinning (i.e., 2008).

Table 4
Fit indices and error statistics calculated from the disk-level model (Eq. 1) and final model (Eq. 2).

Model		AIC	*R*-squared	Model error		
				RMSE	|ME|	|ME| %
Disk-level model	Min.	−140.1	0.056	0.004	0.003	0.98
	Mean	−56.51	0.716	0.015	0.012	3.57
	Max.	−25.65	0.988	0.044	0.033	9.32
Final model		32,918.14	0.386 (0.759)	0.025	0.018	5.23

The value in the parenthesis for the final model indicates the *R*-squared value with both fixed and random terms.

Table 5
Parameter estimates, standard errors (SE), t-values, and standard deviation of the random effect estimates for the final model of ring density given by Eq. 2.

Fixed parameters	Estimate	SE	*t*-value
β_0	0.427	0.024	17.48
β_1	−0.0001	1.59×10^{-5}	−8.52
β_2	−0.041	0.017	−2.37
β_3: h_{disk} 25 %	0.013	0.003	3.94
β_3: h_{disk} 50 %	0.048	0.003	14.25
β_3: h_{disk} 75 %	0.261	0.005	45.88
β_3: h_{disk} BH	0.013	0.003	3.73
β_4	0.011	0.001	5.96
β_5	−3.91	0.202	−19.33
β_6: h_{disk} 25 %	−0.002	0.002	−0.96
β_6: h_{disk} 50 %	−0.028	0.002	−11.64
β_6: h_{disk} 75 %	−0.129	0.003	−32.34
β_6: h_{disk} BH	0.002	0.002	0.97
β_7	0.0009	3.77×10^{-5}	25.16
β_8	−0.0003	2.59×10^{-5}	−12.88
β_9: h_{disk} 25 %	-3.14×10^{-5}	3.76×10^{-5}	−0.83
β_9: h_{disk} 50 %	8.73×10^{-5}	3.79×10^{-5}	2.29
β_9: h_{disk} 75 %	0.0002	4.67×10^{-5}	4.57
β_9: h_{disk} BH	-6.23×10^{-5}	3.83×10^{-5}	−1.62
Random parameters	Std. Dev	Level	
μ_i	0.0276	*Tree*	
μ_{ij}	0.0171	*Disk*	
ε_{ijk}	0.0261	*Residual*	

treatment to 132.48 $m^2 \cdot ha^{-1}$ for the control. Because plots differed in their initial volumes, straightforward comparisons among treatments were most easily made using annual increment and volume increment percentages. Expressed as a percentage relative to the control, the plots with 50 CTR exhibited the highest volume percentage, followed by 100 CTR at the start of two growth periods as well as at the end of the second growth period (2021). In all cases, the volume of thinned plots was always lower than that of the control plot. Nevertheless, the percentage volume changes from 2008 to 2021 were higher for plots thinned from below and 100 CTR than those with 50 CTR (Table 6).

The control plots had the highest annual volume increments for both growth periods, followed by thinning from below for growth period 1 and 50 CTR for growth period 2 (Figs. 3A, 3B). Overall, for 13 years, plots thinned from below exhibited the lowest total growth in volume, with an annual increment of 8.83 $m^3 \cdot ha^{-1}$. Unthinned or control plots demonstrated the highest volume increment at 10.34 $m^3 \cdot ha^{-1} \cdot year^{-1}$, whereas treatments with 100 CTR and 50 CTR had volume increments of 9.36 and 9.54 $m^3 \cdot ha^{-1} \cdot year^{-1}$, respectively (Table 6). At the stand level, we observed no statistical differences in the annual volume increment among the silvicultural treatments for both growth periods and sites (Table 7). Nevertheless, variations were noticeable in the annual volume increment concerning both the SDI and the growth periods (Table 8). As expected, treatments with higher stand density exhibited a higher volume increment, and the SDI rose uniformly for all plots, regardless of the treatment, during the transition from growth period 1 to growth period 2 (Fig. 3). Although statistically insignificant, the annual volume increment rate for plots thinned from below was found to be lower in growth period 2 than in growth period 1, despite an increase in the SDI (Fig. 3).

Our results indicated that changes in stand structure can affect the CO_2 sequestration rate in the stem, with the control treatments storing the most carbon and the thinning from below treatment storing the least (Table 6). The highest annual CO_2 sequestration values for both growth periods were observed in the control plots. The lowest value was found in the 100 CTR plots during growth period 1 and in the plots thinned from below during growth period 2 (Figs. 4A, 4B). Annual CO_2 sequestration across all treatments increased uniformly by approximately 13–14 % from growth period 1 to growth period 2, except for plots thinned from below, which decreased by 6 % (Figs. 4A, 4B).

Throughout the study period, annual CO_2 sequestration in the stem was highest in the control plots, reaching 5.84 $t \cdot ha^{-1} \cdot year^{-1}$, and lowest in the plots thinned from below, with a rate of 4.75 $t \cdot ha^{-1} \cdot year^{-1}$. Plots with 50 CTR showed a slightly higher CO_2 sequestration rate (5.35 $t \cdot ha^{-1} \cdot year^{-1}$) than those with 100 CTR (5.17 $t \cdot ha^{-1} \cdot year^{-1}$) (Table 6). The lack of difference in both annual stem volume increment and stem

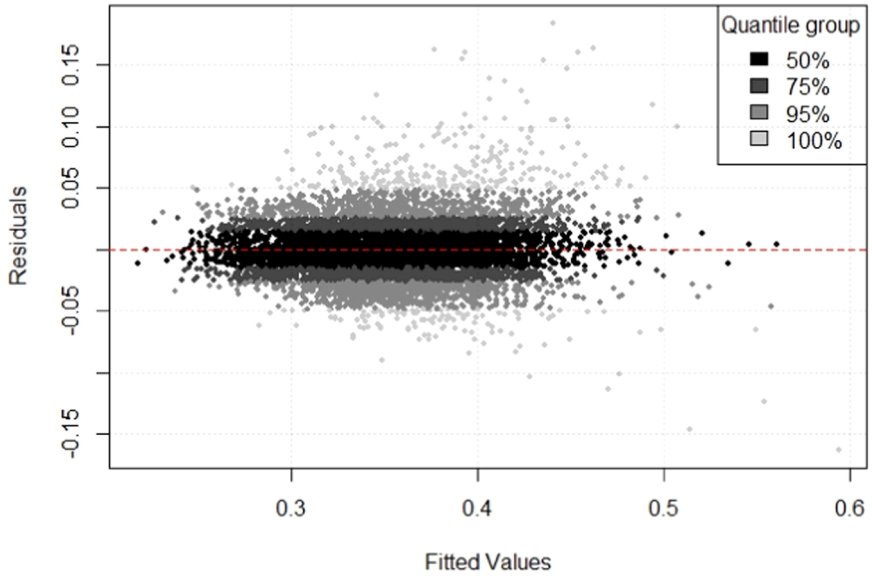

Fig. 2. Model residuals of the final model plotted against the fitted values of ring density. The gray shading level represents the different percentiles of the residuals.

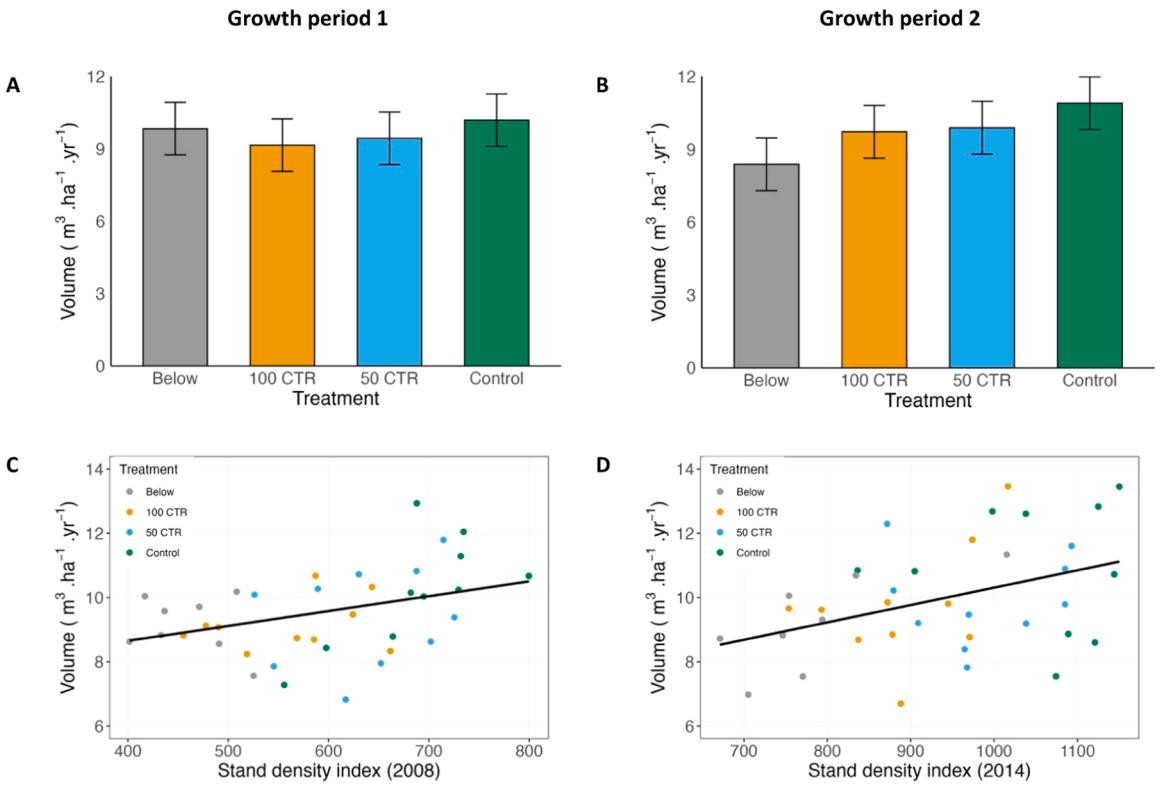

Fig. 3. Figures in the upper row denote the annual volume increment per hectare for four thinning treatments at (A) growth period 1 (2008–2014) and (B) growth period 2 (2014–2021). Error bars are the standard error of the mean. Figures in the lower row represent the annual volume increment per hectare during (C) growth period 1 and (D) growth period 2 as a function of the stand density index (Pretzsch and Biber, 2005) calculated immediately before the start of the respective growth periods.

Table 6
Average tree characteristics (standard deviation in parentheses) of three inventory periods for each thinning treatment and their respective total volume and carbon sequestration in the stems and increment rates during the 13-year study period.

Variable	Thinning type			
	Below	100 CTR	50 CTR	Control
DBH (cm) 2008	13.01 (4.69)	12.28 (4.54)	12.44 (4.23)	12.57 (4.38)
DBH (cm) 2014	15.89 (5.30)	14.72 (5.13)	14.73 (4.86)	14.88 (4.93)
DBH (cm) 2021	17.77 (6.24)	16.27 (6.11)	16.09 (6.11)	16.02 (6.45)
Height (m) 2008	10.18 (2.26)	10.41 (2.26)	10.27 (2.62)	10.35 (2.20)
Height (m) 2014	11.56 (2.54)	11.35 (2.20)	11.22 (2.14)	11.26 (2.00)
Height (m) 2021	12.56 (3.38)	12.44 (3.19)	12.25 (3.22)	12.23 (3.53)
BA ($m^2 \cdot ha^{-1}$) before thinning	26.83	26.72	28.92	29.22
BA ($m^2 \cdot ha^{-1}$) after thinning in 2008	21.51	23.39	27.48	29.22
Total volume ($m^3 \cdot ha^{-1}$) in 2008 as a % of control	69.12 %	82.83 %	92.22 %	100 %
Total volume ($m^3 \cdot ha^{-1}$) in 2014 as a % of control	77.09 %	85.05 %	92.37 %	100 %
Total volume ($m^3 \cdot ha^{-1}$) in 2021 as a % of control	77.30 %	87.27 %	93.23 %	100 %
Annual volume increment during the study period ($m^3 \cdot ha^{-1} \cdot year^{-1}$)	8.83	9.36	9.54	10.34
Annual CO_2 sequestration during the study period ($t \cdot ha^{-1} \cdot year^{-1}$)	4.75	5.17	5.35	5.84

CO_2 sequestration trends among the various treatment plots suggested a minimal effect of density variations between and within the tree stems. The analysis of variance results of CO_2 sequestration among stand structures (silviculture treatments), stand density, and growth periods mirrored the observations for annual volume increment differences: no significant difference was observed between thinning modalities (Table 7), whereas a significant difference was noted between the SDI and growth period (Table 8). The CO_2 sequestration rates for all the plots, except those thinned from below, were found to be higher in growth period 2 than in growth period 1 (Fig. 4).

Total stem CO_2 sequestration over the studied 13 years was estimated with the average wood density at BH (367 $kg \cdot m^{-3}$) closely aligned with the value obtained using the within-tree density variations. The projection based on the average density at BH slightly overestimated total CO_2 sequestration per hectare, ranging from 0.54 % to 4.24 % across various thinning plots (Fig. 5). Interestingly, the distinctions between treatments appeared to be less pronounced when considering the average density at BH. However, the total CO_2 sequestration using the published wood density value (412 $kg \cdot m^{-3}$) for white spruce, as provided by De Araujo et al. (2015), exceeded the actual value by up to 15 % (Fig. 5).

4. Discussion

In the context of climate change, carbon mitigation is more often integrated as explicitly stated forest management and silvicultural

Table 7
F-values (P-values in parentheses) for the analysis of variance of stand-level variables (volume increment and CO_2 sequestration in the stems) with silvicultural treatments (control, thinned from below, thinned by CTR), growth periods (period 1 and period 2), and site.

Source of variation	Response: volume increment			Response: CO_2 sequestration		
	ndf	ddf	*F*-values (*P*-values)	ndf	ddf	*F*-values (*P*-values)
Site	1	71	0.08 (0.77)	1	71	0.70 (0.40)
Treatment	3	71	0.69 (0.56)	3	71	0.72 (0.54)
Growth period	1	71	0.54 (0.46)	1	71	2.39 (0.12)
Treatment x growth period	3	71	1.74 (0.16)	3	71	1.55 (0.20)

Note: ddf, denominator degrees of freedom; ndf, numerator degrees of freedom.

Table 8
F-values (P-values in parentheses) for the analysis of variance of stand-level variables (volume increment and CO_2 sequestration in the stems) with the stand density index (SDI) immediately before the start of the respective growth periods, growth periods (period 1 and period 2), and site.

Source of variation	Response: volume increment			Response: CO_2 sequestration		
	ndf	ddf	*F*-values (*P*-values)	ndf	ddf	*F*-values (*P*-values)
Site	1	75	0.12 (0.72)	1	75	0.01 (0.90)
SDI	1	75	**4.30 (<0.05)**	1	75	**6.30 (<0.05)**
Growth period	1	75	**9.39 (<0.05)**	1	75	**6.42 (<0.05)**
SDI x growth period	1	75	0.37 (0.54)	1	75	0.32 (0.57)

Note: Bold values denote significance at $P < 0.05$; ddf, denominator degrees of freedom; ndf, numerator degrees of freedom.

objectives. In this regard, our study aimed to assess how CTR influences growth ring characteristics and carbon sequestration in the stems of white spruce. The control and thinned treatments exhibited a similar trend in RD chronologies—characterized by a decline until 2008 followed by an upward trend from 2009; thus, it was difficult to attribute the observed relative RD patterns of thinned plots as only a consequence of thinning. Overall, stand productivity, measured by either stem volume or sequestered carbon increment of the stems, was invariant to thinning intensity but increased with SDI. To precisely estimate carbon, we recommend accounting for the density variation between trees by accurately determining the average wood density for each tree. A key implication of our findings is that although reducing stand density to promote individual tree growth may not immediately enhance carbon stocks found in the main stem of the trees, it could potentially recover the lost stock and ultimately lead to a significant increase in total carbon over the long run (Horner et al., 2010; Schaedel et al., 2017).

4.1. *Variations in ring density*

Variation in the radial density of conifers typically exhibits one of the three patterns: a gradual increase in average RD from juvenile wood to mature wood (type I); a high initial density near the pith with a rapid decrease followed by a gradual increase (type II); or a consistent decrease in density from pith to bark (type III) (John, 1980; Schimleck et al., 2022). In this study, the radial variation of wood density showed a type II pattern, typical of spruce (Saranpää, 2003; Alteyrac et al., 2005; Gardiner et al., 2011; Xiang et al., 2014). This type II pattern has been attributed to the higher earlywood density with low earlywood proportion near the pith (Koubaa et al., 2005), which is a clear adaptive strategy of conifers to respond to complex loading patterns, such as wind or snow loads, by providing a more stable structure at a young age (Telewski, 1989; Van Gelder et al., 2006). In the vertical direction, the

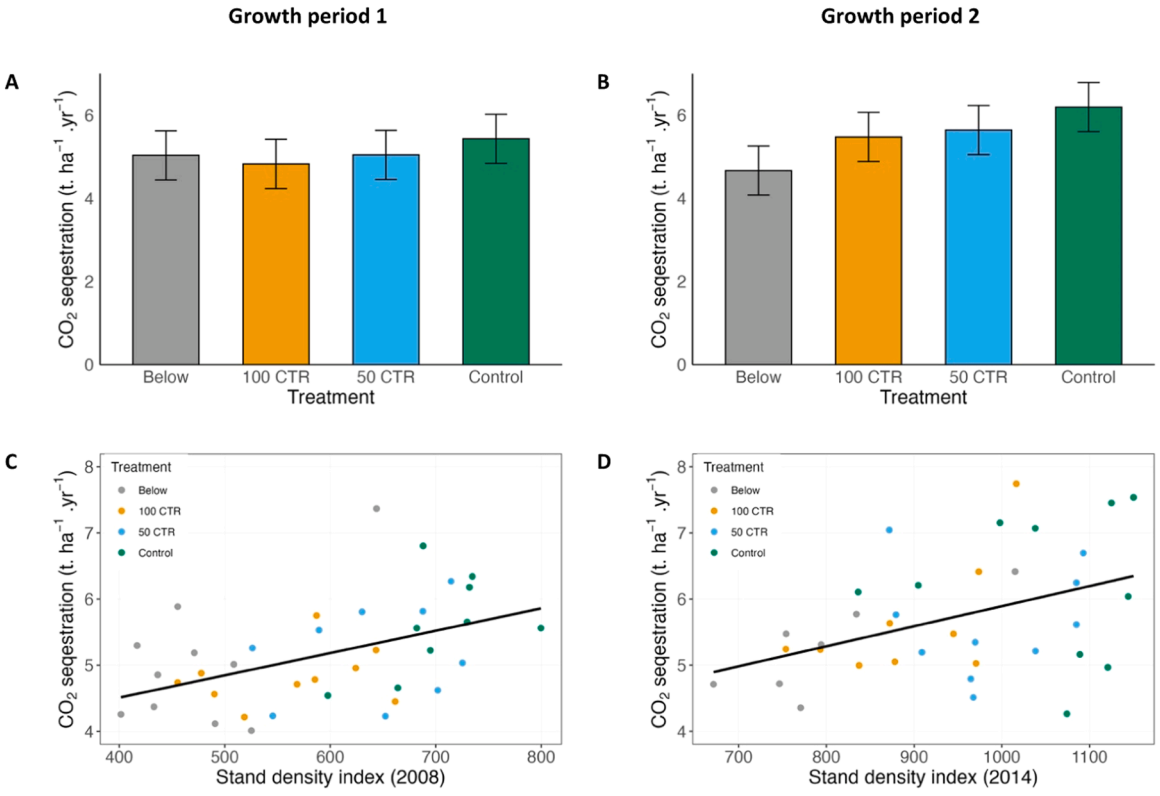

Fig. 4. Figures in the upper row denote annual CO_2 sequestration in the stems per hectare for four thinning treatments at (A) growth period 1 (2008–2014) and (B) growth period 2 (2014–2021). Error bars are the standard error of the mean. Figures in the lower row represent the annual CO_2 sequestration in the stems per hectare during (C) growth period 1 and (D) growth period 2 as a function of the stand density index (Pretzsch and Biber, 2005) calculated immediately before the start of the respective growth periods.

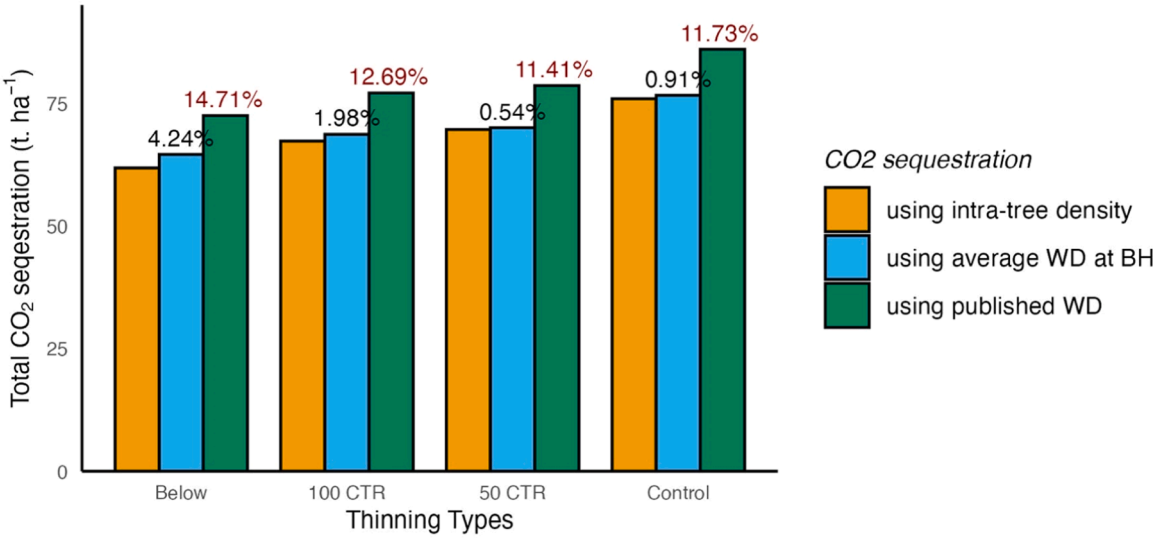

Fig. 5. Total CO_2 sequestration in the stems per hectare over the 13-year study period computed using within-tree density variation, average wood density at breast height, and a published wood density of 412 $kg{\cdot}m^{-3}$ for four thinning types. The numerical values presented above the bars represent the percentage difference between the total CO_2 sequestration in the stems obtained using respective wood density and that derived from within-tree density variations. The WD and BH in the figure represent wood density and breast height, respectively.

mean density exhibited a flattened U-shaped pattern of fluctuation with height, indicating a minimal decline up to one-fourth of the tree's height, followed by a slight rise toward the apex. The U-shaped pattern of vertical density variation has also been reported by Repola (2006) for pine and birch, Wassenberg et al. (2015) for *Quercus,* and Longuetaud et al. (2017) for temperate tree species. This variation occurs because of the proportion of juvenile wood that increases from the base to the top of the tree. Often, the pattern of radial variations of wood density contributes to explaining the vertical trends, as the composition of wood within the stem—whether it is juvenile versus mature wood or the proportion of narrow rings—can vary with tree height. For instance, we observed "pattern a" vertical variation as described by Longuetaud et al. (2017), in which average wood density increases from the bottom to the top of the stem because of the decrease in wood density with distance from the pith. In other words, this occurs when wood density increases along the stem for the same cambial age, likely because of the maturity of the apical meristem (Jyske et al., 2008). Conversely, if density increases from pith to bark, an opposite vertical density pattern would have been evident. Moreover, most of the studied disks had a high proportion of juvenile wood, where the transition to maturity is estimated at 10–20 years (Zobel and Sprague, 2012). Thus, caution is warranted when generalizing the axial density pattern of white spruce solely from our study, as our results were derived from trees having a maximum age of 34 years.

The higher average RD noted for intermediate trees aligns with the conclusions drawn by Lindström (1996) and Deng et al. (2014). The decline in RD as tree dominance increases is observed because trees with slower growth rates tend to develop denser wood (Johansson, 1993; Pape, 1999a). Trees under higher competition produce proportionally more latewood, distinguished by thicker cell walls, a smaller lumen, and increased density (John, 1980; Tsoumis and Panagiotidis, 1980; Peltola et al., 2007). Additionally, Pukkala et al. (1998) and Peltola et al. (2002) found that suppressed trees exhibited a faster and more pronounced response (in relative terms) to thinning than dominant trees, which might explain the observed temporary decrease in the average RD of the intermediate class following thinning. With reduced competition, intermediate trees may have used available resources for quicker but potentially less dense growth, aiming to establish themselves in the canopy.

The response of RD to thinning varies between species. For instance, a slight reduction in wood density has been observed after thinning in Norway spruce (*Picea abies* L.) (Herman et al., 1998; Jaakkola et al., 2005) and Scots pine (*Pinus sylvestris*, L.) (Mörling, 2002), whereas, wood density increased after thinning in loblolly pine (*Pinus taeda* L.) (Megraw, 1985) and red pine (*Pinus resinosa* Sol.) (Paul, 1958). A sudden release from high competition through intense thinning can lead to a temporary drop in wood density (Pape, 1999b). Moreover, a limited change in wood density has been observed following precommercial thinning in black spruce (Tong et al., 2009; Vincent et al., 2011) and Scots pine (Tasissa and Burkhart, 1997; Peltola et al., 2009), results that are in line with ours. Our findings demonstrate that two rings with the same ring width, one from a thinned tree and the other from an unthinned tree, have the same RD values. Thinning-induced alterations in competition and resource availability can lead to diverse growth patterns among the remaining trees (Hannrup et al., 2000), ultimately altering the relationship between RD and RW. Therefore, changes in RD following thinning could be explained by changes in growth rates, such that thinning influences RD indirectly. For instance, thinning results in an increased ring width, which subsequently contributes to a proportional change in RD (Barbour et al., 1994; Schneider et al., 2008). Also, as cambial age increases, there is a tendency for the proportion of latewood to increase, which leads to a corresponding rise in RD toward the bark (Moore, 2011). Koubaa et al. (2000) presented a declining correlation between RD and RW in black spruce as wood transitions from juvenile to mature stages, aligning with the observed rise in RD for the same ring width after thinning.

4.2. *Post-thinning CO_2 sequestration in tree stems*

The effects of thinning on stand-level productivity depend on thinning intensity and the remaining trees' capacity to compensate for the removed carbon through enhanced uptake (Saunders et al., 2012). In our study, during the thinning treatment, the stand densities of the 50 CTR, 100 CTR, and thinning from below plots were reduced by an average of 4 %, 11 %, and 23 %, respectively (Dupont-Leduc et al., 2020). The lower annual volume increment and stem CO_2 sequestration rate observed for the 100 CTR and thinned from below plots are thus attributed to the stand density following thinning. This pattern aligns with findings from other similar studies, indicating that thinning reduces stand density significantly, thereby immediately decreasing net carbon stocks (Dewar and Cannell, 1992; Vesterdal et al., 1995; Campbell et al., 2009; Powers et al., 2011; Ruiz-Peinado et al., 2016; Lin et al.,

2018). Moreover, we found evidence that SDI affects stand-level productivity, with higher stand-level volume increments and stem CO_2 sequestration rates observed in the higher SDI plots. Higher SDI values typically indicate a larger basal area, which can lead to increased CO_2 sequestration through enhanced photosynthetic capacity and a greater biomass accumulation (Waring et al., 2020; Zhao et al., 2022). However, this increased capacity seems to depend on the forest type. In a study of China's forested regions, Wang et al. (2024) reported that increasing SDI reduces biomass and soil organic carbon in natural forests by 231.7 $t \cdot ha^{-1}$, whereas in planted forests, it increases to 74.7 $t \cdot ha^{-1}$, suggesting the need for a forest-type-specific management plan to optimize carbon sequestration. In the case of white spruce plantations, if the goal is to maximize stand-level volume increment or stem CO_2 sequestration, maintaining a higher stand density without thinning would be advisable. It should also be noted that thinning practices may initially reduce stand productivity but ultimately lead to a surge in growth and an increase in sawtimber volume. For instance, Schroeder (1991) reported an 11 % increase in carbon stocks over 50 years in Douglas fir plantations because of thinning, and Balboa-Murias et al. (2006) found that extending rotation, coupled with suitable thinning intensity, could enhance carbon pools in radiata pine. Furthermore, at the beginning of growth period 1, the 100 CTR plots had 82 % of the volume relative to the control, but at the end of growth period 2, they had 87 % of the total volume relative to the control plots, suggesting that the trees are offsetting the volume lost during thinning. Although we did not assess the direct growth changes at the tree level, it has been reported elsewhere that the average diameter increment of residual trees is greater in thinned plots than in unthinned plots (Mäkinen and Isomäki, 2004; Bianchi et al., 2024). The same thinning trial demonstrated that crop trees had improved growth after both CTR and thinning from below over the first five years after thinning relative to those in the unthinned plots (Dupont-Leduc et al., 2020). Thinning effects may take 7–10 years to fully manifest, with thinned stands potentially compensating for initial stock losses by the final rotation. Additionally, thinning enhances forest health and mitigates the risk of climatic uncertainties, such as drought, by reducing stand density (Alvarez et al., 2016; Moreau et al., 2022). Therefore, if forest management aims to achieve an optimal balance between carbon stocks and financial return, the CTR treatment, which minimizes the reduction in stand density and thus increases stem CO_2 sequestration relative to the thinning from below treatment, would be the preferable option.

Current carbon stocks in the tree stem are not the sole indicators of CO_2 sequestration, as the biomass harvested during thinning and other forest carbon pools can substantially contribute to CO_2 sequestration (Perez-Garcia et al., 2005; Lundmark et al., 2014). Marland and Schlamadinger (1997) concluded that optimizing wood product usage to replace more carbon-intensive alternatives results in a clear carbon benefit when compared with a scenario without forest management. Moreover, the amount of carbon stored in non-legacy deadwood—defined as woody debris produced by the current second-growth forest—typically diminishes as the density of the forest stand decreases (Larson et al., 2015; Schaedel et al., 2017). This decline is likely because of the reduced input of woody debris from self-thinning mortality in thinned stands, a trend that becomes more noticeable with the removal of larger trees. If thinning occurs before trees compete and limit each other's growth, the remaining trees quickly fill the space, which results in self-pruning and crown recession (Long et al., 2004). On the other hand, there is limited evidence indicating that the thinning treatments have a substantial effect on legacy carbon pools, which encompass woody debris and forest floor carbon from the pre-existing old-growth forest (Harmon et al., 1986). Given that all the stands are in closed canopy conditions, it is probable that the effect of stand density on decay rates—affected by variations in light and temperature—will be minimal (Harmon et al., 1986). Moreover, belowground biomass, which constitutes about 20 % of the total biomass (Pan et al., 2011), remains relatively stable because of a balance between root mortality following thinning and the compensatory root growth in the residual trees (Zhang et al., 2024, 2018). Thinning affects various aboveground components differently across sites and species because of distinct allocation strategies, with stem biomass typically showing a more pronounced proportional change than branch biomass (Jenkins et al., 2003; Saarinen et al., 2020). Thus, we believe this study provides initial insights into the effects of CTR on carbon dynamics, offering guidance for balancing active forest management with carbon mitigation goals and refining carbon sequestration models. Nevertheless, the carbon dynamics of the forest stand following thinning would be viewed more comprehensively if we integrated the forest carbon pool with the product pool of stored carbon, along with the dead and belowground carbon pools.

In response to the growing concern for natural climate solutions and the gradual acceptance of carbon credit markets, there is an increasing demand for enhanced accuracy in estimating forest carbon levels. The significant overestimates in total CO_2 sequestration, arising from the use of published wood density values, highlight the importance of accounting for the effects of treatments and growing conditions on wood density. For example, Kantavichai et al. (2010) found that the use of the Wood Handbook (Forest Products Laboratory (US), 2021) average density underestimated carbon storage by up to 14 %, whereas the use of biomass equations developed by Gholz et al. (1979) and Jenkins (2004) led to more pronounced underestimates, reaching up to 52 %. In our study, the difference between total CO_2 sequestration estimated using within-tree density variations and average wood density at BH was negligible, with only a noticeable difference for plots thinned from below. However, studies have highlighted significant differences between tree density at BH and average wood density (Wiemann and Williamson, 2014; Kimberley et al., 2015; Longuetaud et al., 2017) and have suggested considering density variations to have more refined carbon estimates (Rueda and Williamson, 1992; Wassenberg et al., 2015). To estimate the CO_2 sequestration, we used only those rings formed after thinning, which exhibited more stable density in both the radial and vertical directions. Often, higher variability in wood density is observed near the pith (Saranpää, 2003); therefore, it is necessary to consider within-tree density variability while estimating carbon gain in all growth years. Furthermore, within-tree density variability patterns and magnitudes are species-specific, with some exhibiting homogeneous variation, whereas others display high variability throughout the stem (Wassenberg et al., 2015). Thus, from our assessment, we recommend sampling wood disks to obtain an accurate estimate of average wood density. If destructive sampling is not possible, sample cores should at least be collected at BH.

5. Conclusions

Our findings offer preliminary evidence to consider a new forest management approach for achieving carbon sequestration objectives. Contrary to our hypothesis, thinning did not significantly affect the annual volume increment and CO_2 sequestration in stems relative to the control plots. The control plots, with a higher stand density, showed a greater annual increment rate; however, thinned plots demonstrated the potential to eventually match the stock level of the control plots over time. These implications suggest that carefully planned thinning interventions have the capacity not only to influence immediate growth dynamics but also to shape the trajectory of carbon sequestration in stems over extended periods. Thinning may not be advisable when the goal is to sequester more carbon, but if necessary, attention should be paid to the timing, intensity, and type of thinning. CTR should be preferred over thinning from below, as the reduction in CO_2 sequestration following CTR was relatively minimal. Moreover, crop trees can yield high-quality wood products that store carbon for 70–100 years, providing a means to offset emissions from fossil fuels (Lindroth et al., 2018). Finding the right balance between thinning intensity and stand-level aboveground net primary productivity requires a compromise that balances an adequate stocking of large dominant trees with

allowing younger trees to grow in the stand. Adopting CTR with moderate stand density reductions could serve as a balanced trade-off, improving the long-term carbon storage potential while mitigating the risk of stand-level net stock loss. This trade-off could also be balanced through early thinning to promote accelerated individual tree growth and encourage the development of understory vegetation from an early stage (He et al., 2012). Additional years of investigation are essential for grasping the long-term effects on carbon stocks in the stem and identifying the point at which stands could recover the carbon loss. For this, the established mixed-effect model could be applied to predict the RD up to the rotational year.

Our study advances conventional carbon estimation methods by integrating differences in site, age, silvicultural treatment, and tree-level attributes by including variations in within-tree and between-tree density. Although our study demonstrates the satisfactory representation of average density at BH for stem carbon estimates, this may not hold when accounting for rings having greater density fluctuations. Including within-tree and between-tree density variations in carbon estimates is not always practical; we therefore recommend obtaining RD measures from a sample of trees that reflect the stand ages and sites being studied.

CRediT authorship contribution statement

Dufour Boris: Writing – review & editing, Visualization, Formal analysis. **Barrette Julie:** Writing – review & editing, Validation, Supervision, Resources, Methodology, Conceptualization. **Mahatara Dipak:** Writing – original draft, Validation, Software, Project administration, Methodology, Investigation, Formal analysis, Conceptualization. **Schneider Robert:** Writing – review & editing, Validation, Supervision, Software, Resources, Methodology, Investigation, Funding acquisition, Data curation, Conceptualization. **Achim Alexis:** Writing – review & editing, Validation, Supervision, Resources. **Sirois Luc:** Writing – review & editing, Validation, Resources, Methodology.

Declaration of Competing Interest

We have no conflicts of competing interest to disclose.

Acknowledgments

This research was funded by Forest Research Service contract number 3329-2019-142332176-B awarded to Robert Schneider by the Ministère des Ressources naturelles et des Forêts (Quebec, Canada) and the Natural Sciences and Engineering Research Council of Canada. The authors acknowledge Laval University and the Institut National de la Recherche Scientifique, Québec, for sample storage and processing. Special thanks to Dr. Pierre Francus for his invaluable advice during data processing and analysis. We also thank the anonymous reviewers for their detailed and insightful feedback, which significantly improved the quality of this paper.

Appendix A. Supporting information

Supplementary data associated with this article can be found in the online version at doi:10.1016/j.foreco.2025.122542.

Data availability

Data will be made available on request.

References

Alteyrac, J., Zhang, S.Y., Cloutier, A., Ruel, J.-C., 2005. Influence of stand density on ring width and wood density at different sampling heights in black spruce (Picea mariana (Mill.) BSP). Wood Fiber Sci. 37, 83–94.

Alvarez, S., Ortiz, C., Díaz-Pinés, E., Rubio, A., 2016. Influence of tree species composition, thinning intensity and climate change on carbon sequestration in Mediterranean mountain forests: a case study using the CO2Fix model. Mitig. Adapt. Strateg. Glob. Change 21, 1045–1058.

Ashton, M.S., Kelty, M.J., 2018. The practice of silviculture: applied forest ecology. John Wiley & Sons.

Auty, D., Achim, A., Macdonald, E., Cameron, A.D., Gardiner, B.A., 2014. Models for predicting wood density variation in Scots pine. For. Int. J. For. Res. 87 (3), 449–458.

Balboa-Murias, M.A., Rodríguez-Soalleiro, R., Merino, A., Álvarez-González, J.G., 2006. Temporal variations and distribution of carbon stocks in aboveground biomass of radiata pine and maritime pine pure stands under different silvicultural alternatives. For. Ecol. Manag. 237 (1-3), 29–38.

Barbour, R.J., Fayle, D.C.F., Chauret, G., Cook, J., Karsh, M.B., Ran, S., 1994. Breast-height relative density and radial growth in mature jack pine (Pinus banksiana) for 38 years after thinning. Can. J. For. Res. 24, 2439–2447.

Bastin, J.-F., Fayolle, A., Tarelkin, Y., Van den Bulcke, J., De Haulleville, T., Mortier, F., Beeckman, H., Van Acker, J., Serckx, A., Bogaert, J., 2015. Wood specific gravity variations and biomass of central African tree species: the simple choice of the outer wood. PLoS One 10, e0142146.

Bianchi, S., Huuskonen, S., Hynynen, J., Niemistö, P., 2024. Comparing wood production and carbon sequestration after extreme thinnings in boreal Scots pine stands. For. Ecol. Manag. 553, 121641.

Bolstad, P.V., Vose, J.M., 2005. Forest and pasture carbon pools and soil respiration in the southern Appalachian Mountains. For. Sci. 51, 372–383.

Briceño-Elizondo, E., Garcia-Gonzalo, J., Peltola, H., Kellomäki, S., 2006. Carbon stocks and timber yield in two boreal forest ecosystems under current and changing climatic conditions subjected to varying management regimes. Environ. Sci. Policy 9 (3), 237–252.

Bronick, C.J., Lal, R., 2005. Soil structure and management: a review. Geoderma 124, 3–22.

Brown, S., 2002. Measuring carbon in forests: current status and future challenges. Environ. Pollut. 116 (3), 363–372.

Bunn, A.G., 2010. Statistical and visual crossdating in R using the dplR library. Dendrochronologia 28, 251–258.

Campbell, J., Alberti, G., Martin, J., Law, B.E., 2009. Carbon dynamics of a ponderosa pine plantation following a thinning treatment in the northern Sierra Nevada. For. Ecol. Manag. 257, 453–463.

Campelo, F., Mayer, K., Grabner, M., 2019. xRing—an R package to identify and measure tree-ring features using X-ray microdensity profiles. Dendrochronologia 53, 17–21.

Chave, J., Andalo, C., Brown, S., Cairns, M.A., Chambers, J.Q., Eamus, D., Fölster, H., Fromard, F., Higuchi, N., Kira, T., Lescure, J.P., 2005. Tree allometry and improved estimation of carbon stocks and balance in tropical forests. Oecologia 145, 87–99.

D'Amato, A.W., Troumbly, S.J., Saunders, M.R., Puettmann, K.J., Albers, M.A., 2011. Growth and survival of Picea glauca following thinning of plantations affected by eastern spruce budworm. North. J. Appl. For. 28 (2), 72–78.

De Araujo, F., Hart, J.F., Mansfield, S.D., 2015. Variation in trembling aspen and white spruce wood quality grown in mixed and single species stands in the boreal mixedwood forest. Forests 6, 1628–1648.

Deng, X., Zhang, L., Lei, P., Xiang, W., Yan, W., 2014. Variations of wood basic density with tree age and social classes in the axial direction within pinus massoniana stems in Southern China. Ann. For. Sci. 71, 505–516.

Dewar, R.C., Cannell, M.G.R., 1992. Carbon sequestration in the trees, products and soils of forest plantations: an analysis using UK examples. Tree Physiol. 11 (1), 49–71.

Downes, G.M., Drew, D.M., 2008. Climate and growth influences on wood formation and utilisation. South. For. 70 (2), 155–167.

Dupont-Leduc, L., Schneider, R., Sirois, L., 2020. Preliminary results from a structural conversion thinning trial in Eastern Canada. J. For. 118 (5), 515–533.

Dwyer, J.M., Fensham, R., Buckley, Y.M., 2010. Restoration thinning accelerates structural development and carbon sequestration in an endangered Australian ecosystem. J. Appl. Ecol. 27 (3), 681–691.

Environnement Canada, A.S., 2015. *Normales climatiques au Canada 1980–2010 (Region d'Amqui). Available online* ⟨https//climate.weather.gc.ca/climate_⟩ Norm.

Eriksson, E., 2006. Thinning operations and their impact on biomass production in stands of Norway spruce and Scots pine. Biomass. Bioenergy 30, 848–854.

Fahey, T.J., Woodbury, P.B., Battles, J.J., Goodale, C.L., Hamburg, S.P., Ollinger, S.V., Woodall, C.W., 2010. Forest carbon storage: ecology, management, and policy. Front. Ecol. Environ. 8 (5), 245–252.

Filipescu, C.N., Lowell, E.C., Koppenaal, R., Mitchell, A.K., 2014. Modeling regional and climatic variation of wood density and ring width in intensively managed Douglas-fir. Can. J. For. Res. 44, 220–229.

Forest products laboratory (US), 2021. Wood Handb. Wood Eng. Mater. (72).

Fortin, M., Bernier, S., Saucier, J.-P., Labbé, F., 2009. Une relation hauteur-diamètre tenant compte de l'influence de la station et du climat pour 20 espèces commerciales du Québec. Gouv. du Québec. Dir. De. la Rech. For. ère.

Franceschini, T., Gauthray-Guyénet, V., Schneider, R., Ruel, J.-C., Pothier, D., Achim, A., 2018. Effect of thinning on the relationship between mean ring density and climate in black spruce (Picea mariana (Mill.) BSP). Internaltional. J. For. Res. 91, 366–381.

Franklin, J.F., Spies, T.A., Van Pelt, R., Carey, A.B., Thornburgh, D.A., Berg, D.R., Lindenmayer, D.B., Harmon, M.E., Keeton, W.S., Shaw, D.C., 2002. Disturbances and structural development of natural forest ecosystems with silvicultural implications, using douglas-fir forests as an example. For. Ecol. Manag. 155, 399–423.

Gagné, L., Sirois, L., Lavoie, L., 2016. Comparison of volume and value of softwoods from downslope and elite tree clearance in eastern Canada. Can. J. For. Res. 46, 1320–1329.

Gagné, L., Sirois, L., Lavoie, L., 2019. Seed rain and seedling establishment of Picea glauca and Abies balsamea after partial cutting in plantations and natural stands. Forests 10, 221.

Garcia-Gonzalo, J., Peltola, H., Briceno-Elizondo, E., Kellomäki, S., 2007. Changed thinning regimes may increase carbon stock under climate change: a case study from a Finnish boreal forest. Clim. Change 81, 431–454.
Gardiner, B., Leban, J.-M., Auty, D., Simpson, H., 2011. Models for predicting wood density of British-grown Sitka spruce. Forestry 84, 119–132.
Geng, Y., Yue, Q., Zhang, C., Zhao, X., von Gadow, K., 2021. Dynamics and drivers of aboveground biomass accumulation during recovery from selective harvesting in an uneven-aged forest. Eur. J. For. Res. 140, 1163–1178.
Gholz, H.L., Grier, C.C., Campbell, A.G., Brown, A.T., 1979. Equations for estimating biomass and leaf area of plants in the Pacific Northwest. Res. Pap. 41, Forestry Research Laboratory, Oregon State University, School of Forestry, Corvallis, 38 pp.
Gong, C., Tan, Q., Liu, G., Xu, M., 2021. Forest thinning increases soil carbon stocks in China. For. Ecol. Manag. 482, 118812.
Gonzalez-Benecke, C.A., Martin, T.A., Cropper Jr, W.P., Bracho, R., 2010. Forest management effects on in situ and ex situ slash pine forest carbon balance. For. Ecol. Manag. 260, 795–805.
Grenon, F., Lussier, J.M., Sirois, L., 2007. Conversion de jeunes forêts du Bas-St-Laurent en peuplements inéquiennes dans un contexte d'aménagement forestier écosystémique. UQAR Serv. Can. Cent. Can. Sur Fibre Bois 80.
Handbook, W., 1999. *Wood Handbook-Wood as an engineering material*. US Department of Agriculture and Forest Service. Forest Production Laboratory, Madison, WI, USA. Gen. Tech. Rep. FPLGTR-113.
Hannrup, B., Ekberg, I., Persson, A., 2000. Genetic correlations among wood, growth capacity and stem traits in Pinus sylvestris. Scand. J. For. Res. 15 (2), 161–170.
Harmon, M.E., Franklin, J.F., Swanson, F.J., Sollins, P., Gregory, S.V., Lattin, J.D., Anderson, N.H., Cline, S.P., Aumen, N.G., Sedell, J.R., 1986. Ecology of coarse woody debris in temperate ecosystems. Adv. Ecol. Res. 15, 133–302.
Harmon, M.E., Hua, C., 1991. Coarse woody debris dynamics in two old-growth ecosystems. Bioscience 41, 604–610.
He, L., Chen, J.M., Pan, Y., Birdsey, R., Kattge, J., 2012. Relationships between net primary productivity and forest stand age in US forests. Glob. Biogeochem. Cycles 26. GB3009.
Herman, M., Dutilleul, P., Avella-Shaw, T., 1998. Growth rate effects on temporal trajectories of ring width, wood density, and mean tracheid length in Norway spruce (Picea abies (L.) Karst.). Woodand Fiber Sci. 30, 6–17.
Hollinger, D.Y., Maclaren, J.P., Beets, P.N., Turland, J., 1993. Carbon sequestration by New Zealand's plantation forests. N. Z. J. For. Sci. 23 (2), 194–208.
Hoover, C., Stout, S., 2007. The carbon consequences of thinning techniques: stand structure makes a difference. J. For. 105 (5), 266–270.
Horner, G.J., Baker, P.J., Mac Nally, R., Cunningham, S.C., Thomson, J.R., Hamilton, F., 2010. Forest structure, habitat and carbon benefits from thinning floodplain forests: managing early stand density makes a difference. For. Ecol. Manag. 259, 286–293.
Ikonen, V.-P., Peltola, H., Wilhelmsson, L., Kilpeläinen, A., Väisänen, H., Nuutinen, T., Kellomäki, S., 2008. Modelling the distribution of wood properties along the stems of Scots pine (Pinus sylvestris L.) and Norway spruce (Picea abies (L.) Karst.) as affected by silvicultural management. For. Ecol. Manag. 256, 1356–1371.
IPCC 1990. the IPCC scientific assessment. Contribution of Working Group I to the First Assessment Report of the Intergovernmental Panel on Climate Change, 365.
IPCC, 2003. Good practice guidance for land use, land-use change and forestry. *Institute for Global Environmental Strategies (IGES)*, Hayama, Japan, pp. 675. [online] URL: ⟨http://www⟩. ipcc-nggip.iges.or.jp/.
IPCC, 2023. Summary for policymakers: synthesis report. Climate Change 2023: Synthesis Report Contribution of Working Groups I, II and III to the Sixth Assessment Report of the Intergovernmental Panel on Climate Change. 1–34.
ISO 554, 2002. *Standard atmospheres for conditioning and/or testing* – specifications. International Organization for Standardization (ISO), Geneva, Switzerland.
Ivković, M., Gapare, W., Wu, H., Espinoza, S., Rozenberg, P., 2013. Influence of cambial age and climate on ring width and wood density in Pinus radiata families. Ann. For. Sci. 70, 525–534.
Jaakkola, T., Mäkinen, H., Saranpää, P., 2005. Wood density in Norway spruce: changes with thinning intensity and tree age. Can. J. For. Res. 35, 1767–1778.
Jandl, R., Lindner, M., Vesterdal, L., Bauwens, B., Baritz, R., Hagedorn, F., Johnson, D. W., Minkkinen, K., Byrne, K.A., 2007. How strongly can forest management influence soil carbon sequestration? Geoderma 137, 253–268.
Jenkins, J.C., 2004. Compr. Database diameter-Based Biomass-.-. Regres. North Am. tree Species U. S. Dep. Agric., For. Serv., Northeast. Res. Station; 2004.
Jenkins, J.C., Chojnacky, D.C., Heath, L.S., Birdsey, R.A., 2003. National-scale biomass estimators for United States tree species. For. Sci. 49 (1), 12–35.
Johansson, K., 1993. Influence of initial spacing and tree class on the basic density of Picea abies. Scand. J. For. Res. 8 (1-4), 18–27.
John, P.A., 1980. *Textbook of wood technology: structure, identification, properties, and uses of the commercial woods of the United States and Canada*. McGraw-Hill series in forest resources (USA).
Johnson, D.W., Curtis, P.S., 2001. Effects of forest management on soil C and N storage: meta analysis. For. Ecol. Manag. 140, 227–238.
Jurgensen, M.F., Harvey, A.E., Graham, R.T., Page-Dumroese, D.S., Tonn, J.R., Larsen, M.J., Jain, T.B., 1997. Impacts of timber harvesting on soil organic matter, nitrogen, productivity, and health of Inland Northwest forests. For. Sci. 43, 234–251.
Jyske, T., Mäkinen, H., Saranpää, P., 2008. Wood density within Norway spruce stems. Silva Fenn. 42 (3), 439–455.
Kantavichai, R., Briggs, D.G., Turnblom, E.C., 2010. Effect of thinning, fertilization with biosolids, and weather on interannual ring specific gravity and carbon accumulation of a 55-year-old Douglas-fir stand in western Washington. Can. J. For. Res. 40, 72–85.
Kariuki, M., 2008. Modelling the impacts of various thinning intensities on tree growth and survival in a mixed species eucalypt forest in central Gippsland, Victoria, Australia. For. Ecol. Manag. 256, 2007–2017.
Kimberley, M.O., Cown, D.J., McKinley, R.B., Moore, J.R., Dowling, L.J., 2015. Modelling variation in wood density within and among trees in stands of New Zealand-grown radiata pine. N. Z. J. For. Sci. 45, 1–13.
Kimura, J., Fujimoto, T., 2014. Modeling the effects of growth rate on the intra-tree variation in basic density in hinoki cypress (Chamaecyparis obtusa). J. Wood Sci. 60, 305–312.
Koubaa, A., Isabel, N., Zhang, S.Y., Beaulieu, J., Bousquet, J., 2005. Transition from juvenile to mature wood in black spruce (Picea mariana (Mill.) BSP). Wood Fiber Sci. 2005 (3), 445–455.
Koubaa, A., Zhang, S.Y., Isabel, N., Beaulieu, J., Bousquet, J., 2000. Phenotypic correlations between juvenile-mature wood density and growth in black spruce. Wood Fiber Sci. 61, 71.
Kurz, W.A., Shaw, C.H., Boisvenue, C., Stinson, G., Metsaranta, J., Leckie, D., Dyk, A., Smyth, C., Neilson, E.T., 2013. Carbon in Canada's boreal forest—a synthesis. Environ. Rev. 21 (4), 260–292.
Laflèche, V., Larouche, C., Guillemette, F., 2013. L'éclaircie commerciale, in: Le Guide Sylvicole Du Québec, Les Concepts et l'application de La Sylviculture. Les Publ. du Québec, Québec 300-327 p.
Larson, A.J., Lutz, J.A., Donato, D.C., Freund, J.A., Swanson, M.E., HilleRisLambers, J., Sprugel, D.G., Franklin, J.F., 2015. Spatial aspects of tree mortality strongly differ between young and old-growth forests. Ecology 96, 2855–2861.
Laurance, W.F., Nascimento, H.E.M., Laurance, S.G., Andrade, A., Ewers, R.M., Harms, K. E., Luizao, R.C.C., Ribeiro, J.E., 2007. Habitat fragmentation, variable edge effects, and the landscape-divergence hypothesis. PLoS One 2, e1017.
Lin, J.-C., Chiu, C.-M., Lin, Y.-J., Liu, W.-Y., 2018. Thinning effects on biomass and carbon stock for young Taiwania plantations. Sci. Rep. 8 (1), 3070.
Lindroth, A., Holst, J., Heliasz, M., Vestin, P., Lagergren, F., Biermann, T., Cai, Z., Mölder, M., 2018. Effects of low thinning on carbon dioxide fluxes in a mixed hemiboreal forest. Agric. For. Meteorol. 262, 59–70.
Lindström, H., 1996. Basic density in Norway spruce, Part III. Development from pith outwards. Wood Fiber Sci. 391–405.
Long, J.N., Dean, T.J., Roberts, S.D., 2004. Linkages between silviculture and ecology: examination of several important conceptual models. For. Ecol. Manag. 200, 249–261.
Longuetaud, F., Mothe, F., Santenoise, P., Diop, N., Dlouha, J., Fournier, M., Deleuze, C., 2017. Patterns of within-stem variations in wood specific gravity and water content for five temperate tree species. Ann. For. Sci. 74, 1–19.
Lundmark, T., Bergh, J., Hofer, P., Lundström, A., Nordin, A., Poudel, B.C., Sathre, R., Taverna, R., Werner, F., 2014. Potential roles of Swedish forestry in the context of climate change mitigation. Forests 5, 557–578.
Mahatara, D., Campelo, F., Houle, L., Caron, A., Barrette, J., Francus, P., Schneider, R., 2024. CTRing: an R package to extract wood density profiles from computed tomography images of discs and logs. Dendrochronologia 88, 126274.
Mäkinen, H., Isomäki, A., 2004. Thinning intensity and growth of Norway spruce stands in Finland. Forestry 77, 349–364.
Mäkinen, H., Saranpää, P., Linder, S., 2002. Wood-density variation of Norway spruce in relation to nutrient optimization and fibre dimensions. Can. J. For. Res. 32, 185–194.
Marland, G., Schlamadinger, B., 1997. Forests for carbon sequestration or fossil fuel substitution? A sensitivity analysis. Biomass. Bioenergy 13, 389–397.
Matthews, G., 1993. Carbon Content trees No 4, 4–21.
Megraw, R.A., 1985. Wood quality factors in loblolly pine: the influence of tree age, position in tree, and cultural practice on wood specific gravity, fiber length, and fibril angle. Tappi Press.
Miller, C., Grayson, S., Houser, A., Clatterbuck, W., Kuers, K., 2010. Thirty-year assessment of released, overtopped white oaks, in: Proceedings of the 17th Central Hardwood Forest Conference, Lexington, KY, USA. pp. 5–7.
Moore, J., 2011. *Wood properties and uses of Sitka spruce in Britain*. Forestry Commission Research Report. Forestry Commission (UK), Edinburgh, 2011.
Moreau, G., Chagnon, C., Achim, A., Caspersen, J., D'Orangeville, L., Sánchez-Pinillos, M., Thiffault, N., 2022. Opportunities and limitations of thinning to increase resistance and resilience of trees and forests to global change. Forestry 95, 595–615.
Mörling, T., 2002. Evaluation of annual ring width and ring density development following fertilisation and thinning of Scots pine. Ann. For. Sci. 59, 29–40.
Muller-Landau, H.C., 2004. Interspecific and inter-site variation in wood specific gravity of tropical trees. Biotropica 36, 20–32.
Nabuurs, G.J., Masera, O., Andrasko, K., Benitez-Ponce, P., Boer, R., Dutschke, M., Elsiddig, E., Ford-Robertson, J., Frumhoff, P., Karjalainen, T., 2007. Forestry. Climate Change 2007: Mitigation. In: Contribution of Working Group III to the Fourth Assessment Report of the Intergovernmental Panel on Climate Change, 2007. Cambridge University Press, Cambridge, pp. 541–584.
Nave, L.E., Vance, E.D., Swanston, C.W., Curtis, P.S., 2010. Harvest impacts on soil carbon storage in temperate forests. For. Ecol. Manag. 259, 857–866.
Nizami, S.M., 2012. The inventory of the carbon stocks in sub tropical forests of Pakistan for reporting under Kyoto Protocol. J. For. Res. 23 (3), 377–384.
Noormets, A., Epron, D., Domec, J.-C., McNulty, S.G., Fox, T., Sun, G., King, J.S., 2015. Effects of forest management on productivity and carbon sequestration: a review and hypothesis. For. Ecol. Manag. 355, 124–140.
Ontl, T.A., Janowiak, M.K., Swanston, C.W., Daley, J., Handler, S., Cornett, M., Hagenbuch, S., Handrick, C., McCarthy, L., Patch, N., 2020. Forest management for carbon sequestration and climate adaptation. J. For. 118 (1), 86–101.
Ortega Rodriguez, D.R., Tomazello-Filho, M., 2019. Clues to wood quality and production from analyzing ring width and density variabilities of fertilized Pinus taeda trees. N. For. 50, 821–843.

Pan, Y., Birdsey, R.A., Fang, J., Houghton, R., Kauppi, P.E., Kurz, W.A., Phillips, O.L., Shvidenko, A., Lewis, S.L., Canadell, J.G., 2011. A large and persistent carbon sink in the world's forests. Science 333, 988–993.
Pape, R., 1999b. Effects of thinning regime on the wood properties and stem quality of Picea abies. Scand. J. For. Res. 14 (1), 38–50.
Pape, R., 1999a. Effects of thinning on wood properties of Norway spruce on highly productive sites. PhD Thesis. Swedish University of Agriculture Science, Uppsala, Sweden.
Paul, B.H., 1958. Specific gravity changes in southern pines after release. South. Lumberm. 163, 122–124.
Peltola, H., Gort, J., Pulkkinen, P., Zubizarreta Gerendiain, A., Karppinen, J., Ikonen, V.-P., 2009. Differences in growth and wood density traits in Scots pine (Pinus sylvestris L.) genetic entries grown at different spacing and sites. Silva Fenn. 43, 192.
Peltola, H., Kilpeläinen, A., Sauvala, K., Räisänen, T., Ikonen, V.-P., 2007. Effects of early thinning regime and tree status on the radial growth and wood density of Scots pine. Silva Fenn. 41, 489–505.
Peltola, H., Miina, J., Rouvinen, I., Kellomäki, S., 2002. Effect of early thinning on the diameter growth distribution along the stem of Scots pine. Silva Fenn. 36, 523.
Perez-Garcia, J., Lippke, B., Comnick, J., Manriquez, C., 2005. An assessment of carbon pools, storage, and wood products market substitution using life-cycle analysis results. Wood Fiber Sci. 2005 140–148.
Pinheiro, J., 2009. nlme: linear and nonlinear mixed effects models. R. Package Version 3, 1–96 (http://cran. r-project. org/web/packages/nlme/).
Powers, M., Kolka, R., Palik, B., McDonald, R., Jurgensen, M., 2011. Long-term management impacts on carbon storage in Lake States forests. For. Ecol. Manag. 262, 424–431.
Prégent, G., Picher, G., Auger, I., 2010. Tarif de cubage, tables de rendement et modèles de croissance pour les plantations d'épinette blanche au Québec. Gouvernement du Québec, Ministère des Ressources naturelles et de la Faune, Direction de la recherche forestière. *Mémoire de recherche foresti*.
Pretzsch, H., Biber, P., 2005. A re-evaluation of Reineke's rule and stand density index. For. Sci. 51, 304–320.
Pukkala, T., Miina, J., Kellomäki, S., 1998. Response to different thinning intensities in young Pinus sylvestris. Scand. J. For. Res. 13, 141–150.
Repola, J., 2006. Models for vertical wood density of Scots pine, Norway spruce and birch stems, and their application to determine average wood density. Silva Fenn. 40, 322.
Rueda, R., Williamson, G.B., 1992. Radial and vertical wood specific gravity in Ochroma pyramidale (Cav. ex Lam.) Urb.(Bombacaceae). Biotropica 512–518.
Ruiz-Peinado, R., Bravo-Oviedo, A., López-Senespleda, E., Montero, G., Río, M., 2013. Do thinnings influence biomass and soil carbon stocks in Mediterranean maritime pinewoods? Eur. J. For. Res. 132, 253–262.
Ruiz-Peinado, R., Bravo-Oviedo, A., Montero, G., Del Río, M., 2016. Carbon stocks in a scots pine afforestation under different thinning intensities management. Mitig. Adapt. Strateg. Glob. Change 21, 1059–1072.
Russo, D., Marziliano, P.A., Macri, G., Proto, A.R., Zimbalatti, G., Lombardi, F., 2019. Does thinning intensity affect wood quality? An analysis of Calabrian Pine in Southern Italy using a non-destructive acoustic method. Forests 10, 303.
Saarinen, N., Kankare, V., Yrttimaa, T., Viljanen, N., Honkavaara, E., Holopainen, M., Hyyppä, J., Huuskonen, S., Hynynen, J., Vastaranta, M., 2020. Assessing the effects of thinning on stem growth allocation of individual Scots pine trees. For. Ecol. Manag. 474, 118344.
Saranpää, P., 2003. Wood density and growth. Wood Qual. its Biol. basis 87–117.
Saunders, M., Tobin, B., Black, K., Gioria, M., Nieuwenhuis, M., Osborne, B.A., 2012. Thinning effects on the net ecosystem carbon exchange of a Sitka spruce forest are temperature-dependent. Agric. For. Meteorol. 157, 1–10.
Schaedel, M.S., Larson, A.J., Affleck, D.L.R., Belote, R.T., Goodburn, J.M., Page-Dumroese, D.S., 2017. Early forest thinning changes aboveground carbon distribution among pools, but not total amount. For. Ecol. Manag. 389, 187–198.
Schimleck, L.R., Dahlen, J., Auty, D., 2022. Radial patterns of specific gravity variation in North American conifers. Can. J. For. Res. 52, 889–900.
Schneider, R., Zhang, S.Y., Swift, D.E., Begin, J., Lussier, J.-M., 2008. Predicting selected wood properties of jack pine following commercial thinning. Can. J. For. Res. 38, 2030–2043.
Schroeder, P., 1991. Can intensive management increase carbon storage in forests? Environ. Manag. 15, 475–481.
Singer, M.T., Lorimer, C.G., 1997. Crown release as a potential old-growth restoration approach in northern hardwoods. Can. J. For. Res. 27, 1222–1232.
Tasissa, G., Burkhart, H.E., 1997. Modeling thinning effects on ring width distribution in loblolly pine (Pinus taeda). Can. J. For. Res. 27, 1291–1301.
Telewski, F.W., 1989. Structure and function of flexure wood in Abies fraseri. Tree Physiol. 5, 113–121.
Tong, Q.-J., Fleming, R.L., Tanguay, F., Zhang, S.Y., 2009. Wood and lumber properties from unthinned and precommercially thinned black spruce plantations. Wood Fiber Sci. 2009 (2), 168–179.
Trimble, G.R., 1971. Early crop-tree release in even-aged stands of Appalachian hardwoods (Vol. 203). Northeastern Forest Experiment Station.
Tsoumis, G., Panagiotidis, N., 1980. Effect of growth conditions on wood quality characteristics of black pine (Pinus nigra Arn.). Wood Sci. Technol. 14 (4), 301–310.
Van Gelder, H.A., Poorter, L., Sterck, F.J., 2006. Wood mechanics, allometry, and life-history variation in a tropical rain forest tree community. N. Phytol. 171, 367–378.
Vesterdal, L., Dalsgaard, M., Felby, C., Raulund-Rasmussen, K., Jørgensen, B.B., 1995. Effects of thinning and soil properties on accumulation of carbon, nitrogen and phosphorus in the forest floor of Norway spruce stands. For. Ecol. Manag. 77, 1–10.
Vieilledent, G., Fischer, F.J., Chave, J., Guibal, D., Langbour, P., Gérard, J., 2018. New formula and conversion factor to compute basic wood density of tree species using a global wood technology database. Am. J. Bot. 105 (10), 1653–1661.
Vincent, M., Krause, C., Koubaa, A., 2011. Variation in black spruce (Picea mariana (Mill.) BSP) wood quality after thinning. Ann. For. Sci. 68, 1115–1125.
Wang, T., Dong, L., Liu, Z., 2024. Factors driving carbon accumulation in forest biomass and soil organic carbon across natural forests and planted forests in China. Front. For. Glob. Change 6, 1333868.
Ward, J.S., 2002. Crop tree release increases growth of mature red oak sawtimber. North. J. Appl. For. 19 (4), 149–154.
Ward, J.S., 2013. Precommercial crop tree release increases upper canopy persistence and diameter growth of oak saplings. North. J. Appl. For. 30 (4), 156–163.
Waring, B., Neumann, M., Prentice, I.C., Adams, M., Smith, P., Siegert, M., 2020. Forests and decarbonization–roles of natural and planted forests. Front. For. Glob. Change 3, 534891.
Wassenberg, M., Chiu, H.-S., Guo, W., Spiecker, H., 2015. Analysis of wood density profiles of tree stems: incorporating vertical variations to optimize wood sampling strategies for density and biomass estimations. Trees 29, 551–561.
Wiemann, M.C., Williamson, G.B., 1989. Radial gradients in the specific gravity of wood in some tropical and temperate trees. For. Sci. 35, 197–210.
Wiemann, M.C., Williamson, G.B., 2014. Wood specific gravity variation with height and its implications for biomass estimation. USDA For. Serv. For. Prod. Lab. Res. Pap. 1–12. FPL-RP-677, 2014; 12 p., 677.
Williamson, G.B., Wiemann, M.C., 2010. Measuring wood specific gravity… correctly. Am. J. Bot. 97, 519–524.
Xiang, W., Leitch, M., Auty, D., Duchateau, E., Achim, A., 2014. Radial trends in black spruce wood density can show an age-and growth-related decline. Ann. For. Sci. 71, 603–615.
Zhang, S.Y., 1995. Effect of growth rate on wood specific gravity and selected mechanical properties in individual species from distinct wood categories. Wood Sci. Technol. 29, 451–465.
Zhang, X., Guan, D., Li, W., Sun, D., Jin, C., Yuan, F., Wang, A., Wu, J., 2018. The effects of forest thinning on soil carbon stocks and dynamics: a meta-analysis. For. Ecol. Manag. 429, 36–43.
Zhang, C., Ju, W., Chen, J.M., Wang, X., Yang, L., Zheng, G., 2015. Disturbance-induced reduction of biomass carbon sinks of China's forests in recent years. Environ. Res. Lett. 10 (11), 114021.
Zhang, H., Liu, S., Yu, J., Li, J., Shangguan, Z., Deng, L., 2024. Thinning increases forest ecosystem carbon stocks. For. Ecol. Manag. 555, 121702.
Zhang, H., Zhou, G., Wang, Y., Bai, S., Sun, Z., Berninger, F., Bai, Y., Penttinen, P., 2019. Thinning and species mixing in Chinese fir monocultures improve carbon sequestration in subtropical China. Eur. J. For. Res. 138, 433–443.
Zhao, M., Sun, M., Xiong, T., Tian, S., Liu, S., 2022. On the link between tree size and ecosystem carbon sequestration capacity across continental forests. Ecosphere 13, e4079.
Zhou, D., Zhao, S.Q., Liu, S., Oeding, J., 2013. A meta-analysis on the impacts of partial cutting on forest structure and carbon storage. Biogeosciences 10, 3691–3703.
Zobel, B.J., Sprague, J.R., 2012. Juvenile wood in forest trees. Springer Science & Business Media.
Zobel, B.J., Van Buijtenen, J.P., 2012. Wood variation: its causes and control. Springer Science & Business Media.
Zubizarreta Gerendiain, A., Peltola, H., Pulkkinen, P., Jaatinen, R., Pappinen, A., Kellomäki, S., 2007. Differences in growth and wood property traits in cloned Norway spruce (Picea abies). Can. J. For. Res. 37 (12), 2600–2611.